Phenotypic models of T cell activation

Article *in* Nature reviews. Immunology · August 2014

DOI: 10.1038/nri3728 · Source: PubMed

4 authors, including:

Philip Anton van der Merwe
University of Oxford
268 PUBLICATIONS **10,486** CITATIONS

SEE PROFILE

Phenotypic models of T cell activation

Melissa Lever[1], Philip K. Maini[2], P. Anton van der Merwe[1] and Omer Dushek[1,2]

Abstract | T cell activation is a crucial checkpoint in adaptive immunity, and this activation depends on the binding parameters that govern the interactions between T cell receptors (TCRs) and peptide–MHC complexes (pMHC complexes). Despite extensive experimental studies, the relationship between the TCR–pMHC binding parameters and T cell activation remains controversial. To make sense of conflicting experimental data, a variety of verbal and mathematical models have been proposed. However, it is currently unclear which model or models are consistent or inconsistent with experimental data. A key problem is that a direct comparison between the models has not been carried out, in part because they have been formulated in different frameworks. For this Analysis article, we reformulated published models of T cell activation into phenotypic models, which allowed us to directly compare them. We find that a kinetic proofreading model that is modified to include limited signalling is consistent with the majority of published data. This model makes the intriguing prediction that the stimulation hierarchy of two different pMHC complexes (or two different TCRs that are specific for the same pMHC complex) may reverse at different pMHC concentrations.

Dissociation time
(τ). The characteristic duration of a T cell receptor–peptide–MHC binding interaction ($\tau = 1/k_{off}$; with typical units of s).

Off-rate
(k_{off}). The rate of T cell receptor–peptide–MHC unbinding (with typical units of s^{-1}).

Potency
(EC_{50}). The concentration or dose of peptide–MHC ligand that produces a half-maximal T cell response (with units provided by the ligand dose).

[1]*Sir William Dunn School of Pathology, University of Oxford, South Parks Road, Oxford, Oxfordshire OX1 3RE, UK.*
[2]*Wolfson Centre for Mathematical Biology, Mathematical Institute, University of Oxford, Oxford, Oxfordshire OX2 6GG, UK.*
Correspondence to O.D.
e-mail:
omer.dushek@path.ox.ac.uk
doi:10.1038/nri3728

T cells initiate and regulate adaptive immune responses to infections and cancer, and have crucial roles in allergy, autoimmunity and transplant rejection[1]. These T cell functions rely on productive binding between T cell receptors (TCRs) and antigens, which are typically short peptides bound to MHC molecules that are displayed on the surface of a variety of cells referred to as antigen-presenting cells (APCs). Upon activation, T cells may proliferate, differentiate, release cytokines, kill target cells and carry out other effector functions. By measuring these functional T cell responses to a variety of peptide–MHC (pMHC) ligands, experiments have established that T cell activation is determined by the TCR–pMHC binding parameters. Despite extensive experimental and mathematical work, we do not currently have a model relating the TCR–pMHC binding interaction to T cell activation that is consistent with the published data.

Experiments using panels of different TCRs and pMHC complexes have reported various relationships between the TCR–pMHC binding parameters and T cell activation, as measured by downstream functional readouts such as cytokine secretion[2–16] (FIG. 1). Several studies have reported that T cell activation has an optimum when plotted over the TCR–pMHC dissociation time (τ)[7–9], which is the reciprocal of the off-rate ($k_{off} = 1/\tau$), and this optimum has been observed *in vivo*[12,17]. Interestingly, one study suggested that the optimum is lost at high pMHC doses[11]. Experiments using detailed pMHC titrations have shown that the potency (EC_{50}) does not exhibit an optimum and is directly correlated with the TCR–pMHC dissociation constant (K_d)[2,4–6,13]. In these dose–response assays, it was found that the maximal efficacy (E_{max}) exhibits a negative correlation with k_{off} (REFS 6,13,16).

These experimental studies highlight that the relationship between the TCR–pMHC binding parameters and T cell activation may be complex (FIG. 1). Over the years, these intriguing observations have, in part, motivated the formulation of a variety of models that aimed to reproduce the observed T cell activation phenotypes[8,11,13,18–24]. However, it is presently unclear which model best describes the published experimental data. One reason for this is that these models have been formulated using different mathematical frameworks that make different biochemical assumptions and, as with the experiments, have provided different readouts of T cell activation. This means that when experimental data are generated, it is often unclear which model or models are consistent and which are inconsistent with the data.

For this Analysis article, we compared all of the published models that have aimed to relate the TCR–pMHC binding parameters to T cell activation. We find that the model that is most consistent with published experimental data is a kinetic proofreading model that includes limited signalling. Our Analysis article highlights the need for additional quantitative experimental data to establish a more definitive model.

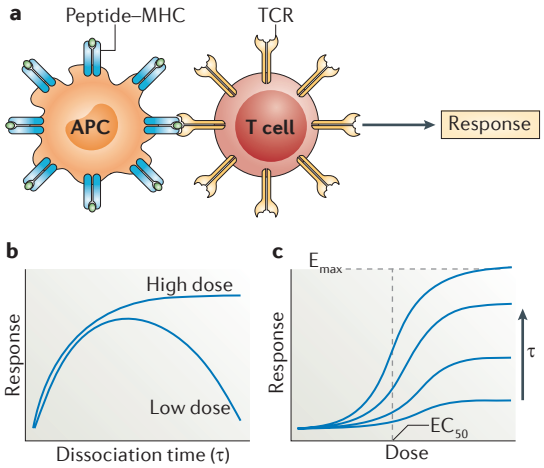

Figure 1 | **Relationship between TCR–pMHC binding parameters and T cell activation.** **a** | A schematic illustrating typical T cell activation assays, in which a functional T cell response (for example, cytokine production) is measured after several hours of interaction with antigens that are presented by antigen-presenting cells (APCs) or by an APC surrogate (not shown). **b** | Experiments have suggested that the T cell response exhibits a maximum when plotted over the dissociation time (τ), such that antigens that bind with long dissociation times (high affinities) lead to poor activation of T cells[7–9,12,17], with one study suggesting that this optimum may only exist at low antigen doses[11]. **c** | Experiments using detailed antigen titration have also shown that the dissociation time determines both the potency (EC_{50}) and maximal efficacy (E_{max}), such that antigens with short dissociation times cannot produce the same maximal response as antigens with long dissociation times[6,13]. Recent data have also suggested the existence of an optimal antigen dose for T cell activation (not shown)[39,40]. Note that panels **b** and **c** are schematics.

Phenotypic models

We carried out an analysis of published models that have aimed to predict the quantitative T cell response to antigens of varying affinities. To directly compare these published models, we recast them using the same mathematical framework into phenotypic models, which are models that aim to make a minimal set of assumptions to capture a cellular phenotype (BOX 1). The mathematical framework is based on standard biochemical reactions in the steady state, which is a reasonable assumption for comparisons with prolonged T cell activation assays (lasting >4 hours; see Supplementary information S1). Five distinct models were identified (FIGS 2,3), including the basic occupancy and kinetic proofreading models, and three modified kinetic proofreading models.

Occupancy model. The occupancy model (also known as the affinity model) posits that T cell activation is proportional to the number of TCRs that are occupied by pMHC complexes (FIG. 2a). In this model, the TCR is assumed to achieve a signalling-competent state immediately upon pMHC binding. The fraction of bound TCRs over the dissociation time and ligand number (FIG. 2b,c) highlights that pMHC complexes with short dissociation times can produce responses that are identical to those with long dissociation times (high affinities), provided that they can be presented at sufficiently high concentrations. The model predicts that pMHC potency (EC_{50}) is directly related to the dissociation time, and therefore to the TCR–pMHC dissociation constant (K_d) (FIG. 2c). The majority of evidence in support of the occupancy model has come from studies that have found a strong correlation between EC_{50} and K_d (REFS 2,4,5,20). The model predicts that the maximum response (E_{max}) is independent of the TCR–pMHC binding parameters, such as the dissociation time (FIG. 2c), which is inconsistent with experimental data[13].

Kinetic proofreading model. The kinetic proofreading model was first put forward to explain how a T cell could discriminate between ligands on the basis of the dissociation time of the ligand–receptor interaction[18]. It proposes that T cell activation is proportional not to the total number of occupied TCRs, but to the fraction of TCRs that have been bound by pMHC complexes for a sufficient duration to allow the TCR to achieve a signalling-competent state (FIG. 2d). In this model, biochemical modifications to the TCR that are required to achieve the signalling-competent state — such as tyrosine phosphorylation by LCK or binding by ζ-chain-associated protein kinase of 70 kDa (ZAP70) — are initiated upon pMHC binding and are immediately reversed upon pMHC unbinding. The delay between pMHC binding and TCR signalling allows T cells to discriminate between pMHC ligands on the basis of their dissociation time from the TCR. The fraction of TCRs in the signalling-competent state over the dissociation time and ligand number (FIG. 2e,f) highlights that maximum activation will be dependent on the dissociation time, which has been experimentally observed[6,13,16]. Therefore, this model implies that antigens with short dissociation times cannot attain responses that are equivalent to those triggered by antigens with long dissociation times by simply increasing their concentrations. Interestingly, the kinetic proofreading model also predicts the correlation between EC_{50} and K_d (FIG. 2i), and therefore all evidence supporting the occupancy model also supports the kinetic proofreading model.

Kinetic proofreading with limited signalling model. As a result of assuming reversible binding between TCRs and pMHC complexes, both of the models that have been considered so far allow for a single pMHC complex to serially bind multiple TCRs. Why then does the present kinetic proofreading model not exhibit an optimum dissociation time for T cell activation, as reported by serial triggering models[13,19,25–28]? The two models make identical biochemical assumptions but differ in the predictor used for T cell activation. Serial triggering models assume that T cell activation is proportional to the rate of forming signalling-competent TCRs, rather than their concentration. This assumption translates into presuming that each TCR can only produce a single 'packet' of signalling per pMHC binding event, and therefore

Dissociation constant (K_d). The characteristic strength of binding ($K_d = k_{off}/k_{on}$; with typical units of μM for three-dimensional solution measurements and typical units of μm^{-2} for two-dimensional membrane measurements).

Maximal efficacy (E_{max}). The maximal T cell response achieved at saturating peptide–MHC concentrations (with units provided by the functional assay).

Box 1 | **Phenotypic models**

Mechanistic models of T cell activation that capture signalling events from T cell receptor triggering to transcriptional regulation are based on many assumptions. These assumptions include which proteins are involved in the process, how they interact with one another, and a variety of parameter values, such as reaction rate constants and protein concentrations. Ultimately, this means that predictions using these models may have high uncertainty and it is not clear how this problem could be resolved.

In contrast to mechanistic models, phenotypic models aim to reproduce experimental data on the basis of a minimal set of assumptions. As they do not capture all signalling events, phenotypic models are deemed effective models. By virtue of making only a few assumptions, phenotypic models have only a few unknown parameters. A key advantage of these models is that it is often obvious (and intuitive) which model assumption is responsible for a particular phenotype. A recent article has highlighted the use of such minimal models[97]. Interestingly, these minimal phenotypic models have been able to reproduce the quantitative T cell phenotypes, despite the large and complex T cell signalling machinery[13,24].

prevents continuous signalling by pMHC complexes with long dissociation times. Put another way, serial triggering models implicitly assume that signalling through individual TCRs is limited.

The kinetic proofreading with limited signalling model is an extension of the kinetic proofreading model positing that TCRs that have reached the signalling-competent state signal for a limited period of time (FIG. 2g). Mechanistically, this assumption is consistent with the observation that TCR signalling is limited to the transit of TCRs from the periphery to the centre of the immunological synapse[29,30], and/or that the TCRs cease to signal once they are tagged for removal from the T cell surface[31–33].

In this model, the predicted activation has an optimum when plotted over the dissociation time (FIG. 2h) even at high ligand concentrations, which is exemplified by the optimum in E_{max} (FIG. 2i). Why does an optimum dissociation time persist at high concentrations? In this model, limited signalling means that in order to maintain continuous (steady-state) signalling — which is required for T cell activation — pMHC complexes must serially bind TCRs. It follows that pMHC ligands with long dissociation times will ultimately remain bound to non-signalling TCRs after producing only transient signalling, at all pMHC concentrations. This is the underlying mechanism for the optimum T cell activation in serial triggering models[13,19,25–28].

Kinetic proofreading with sustained signalling model. The kinetic proofreading with limited signalling model predicts that there will be an optimal dissociation time for T cell activation at all pMHC concentrations. This is inconsistent with some modified kinetic proofreading models that predict an optimum at low but not high pMHC concentrations[8,11]. Instead of assuming that signalling is limited, these models make the assumption that signalling-competent TCRs can sustain signalling following their dissociation from pMHC complexes.

The kinetic proofreading with sustained signalling model is an extension of the kinetic proofreading model that allows signalling-competent TCRs to sustain signalling for a prescribed period of time, even after pMHC unbinding (FIG. 2j). The possibility of a sustained signalling state was inferred from experimental data[8,11], and may be mechanistically related to the idea that TCRs and associated complexes (known as signalosomes) continue to signal following pMHC dissociation until phosphatases dephosphorylate the signalling-competent TCRs or until they are internalized.

The fraction of signalling-competent TCRs over the dissociation time reveals a concentration-dependent optimum (FIG. 2k). At low concentrations, the balance between serial binding and kinetic proofreading means that there will be an optimal dissociation time for a single pMHC complex to produce multiple TCRs with sustained signalling. As signalling is not limited in this model, there is no requirement for serial binding and therefore, at high concentrations, even pMHC complexes with long dissociation times produce maximal signalling. Put differently, the appearance of the optimum is not a result of requiring serial triggering but is a byproduct of it. Animations comparing this model to the three models discussed above underline this difference (see Further information).

The fraction of signalling-competent TCRs over the number of ligands (FIG. 2l) reveals that, like the occupancy model, this model predicts that the E_{max} will be independent of the dissociation time. This puzzling result can be understood as a breakdown in kinetic proofreading. Although signalling-competent TCRs generated by pMHC complexes with short dissociation times are produced at a slow rate (as a result of kinetic proofreading), many such TCRs can be produced and maintained when the concentration of pMHC complexes is sufficiently high. Sustained signalling prevents TCRs from returning to their basal state, which results in a breakdown of kinetic proofreading.

Kinetic proofreading with negative feedback model. The kinetic proofreading with negative feedback model is an extension of the kinetic proofreading model that allows for adjustment of the rate of modification of TCRs at intermediate stages and/or TCRs in the final signalling-competent state. Mechanistically, it is thought that negative feedback may involve SH2 domain-containing protein tyrosine phosphatase 1 (SHP1; also known as PTPN6) being phosphorylated and recruited to the TCR by active LCK that is associated with the phosphorylated TCR[34]. We note that other phosphatases — such as SHP2 (also known as PTPN11), dual-specificity protein phosphatase 6 and others that are under the control of the microRNA miR-181a — may also be involved in this feedback[35]. Unlike all of the models discussed so far, this model predicts that T cell activation will exhibit an optimum as a function of the pMHC dose (FIG. 3). The maximum response and the pMHC concentration producing a half-maximal response in this model are modulated by the dissociation time. This model was initially formulated with both positive and negative feedback using deterministic model calculations[23], and subsequently investigated using stochastic model simulations[36,37]. Recently, a phenotypic reformulation of the model was carried out — which we have used in the present work — illustrating that the main feature of the model can be reproduced with a single negative feedback loop[24].

Immunological synapse
A stable region of contact between a T cell and an antigen-presenting cell that forms through the interaction of adhesion molecules on the surface of both cells. The mature immunological synapse contains two distinct stable membrane domains: a central cluster of T cell receptors known as the central supramolecular activation cluster (cSMAC) and a surrounding ring of adhesion molecules known as the peripheral supramolecular activation cluster (pSMAC).

Deterministic model calculations
Mathematical models in which the mean behaviour of a biochemical reaction network is directly calculated, often using ordinary differential equations. All mathematical models in this Analysis article are of this type.

Stochastic model simulations
Mathematical models in which the behaviour of a biochemical reaction network is simulated on the basis of reaction probabilities. Each simulation produces a different result but the mean of many such simulations often (but not always) agrees with the mean that is directly calculated in deterministic models.

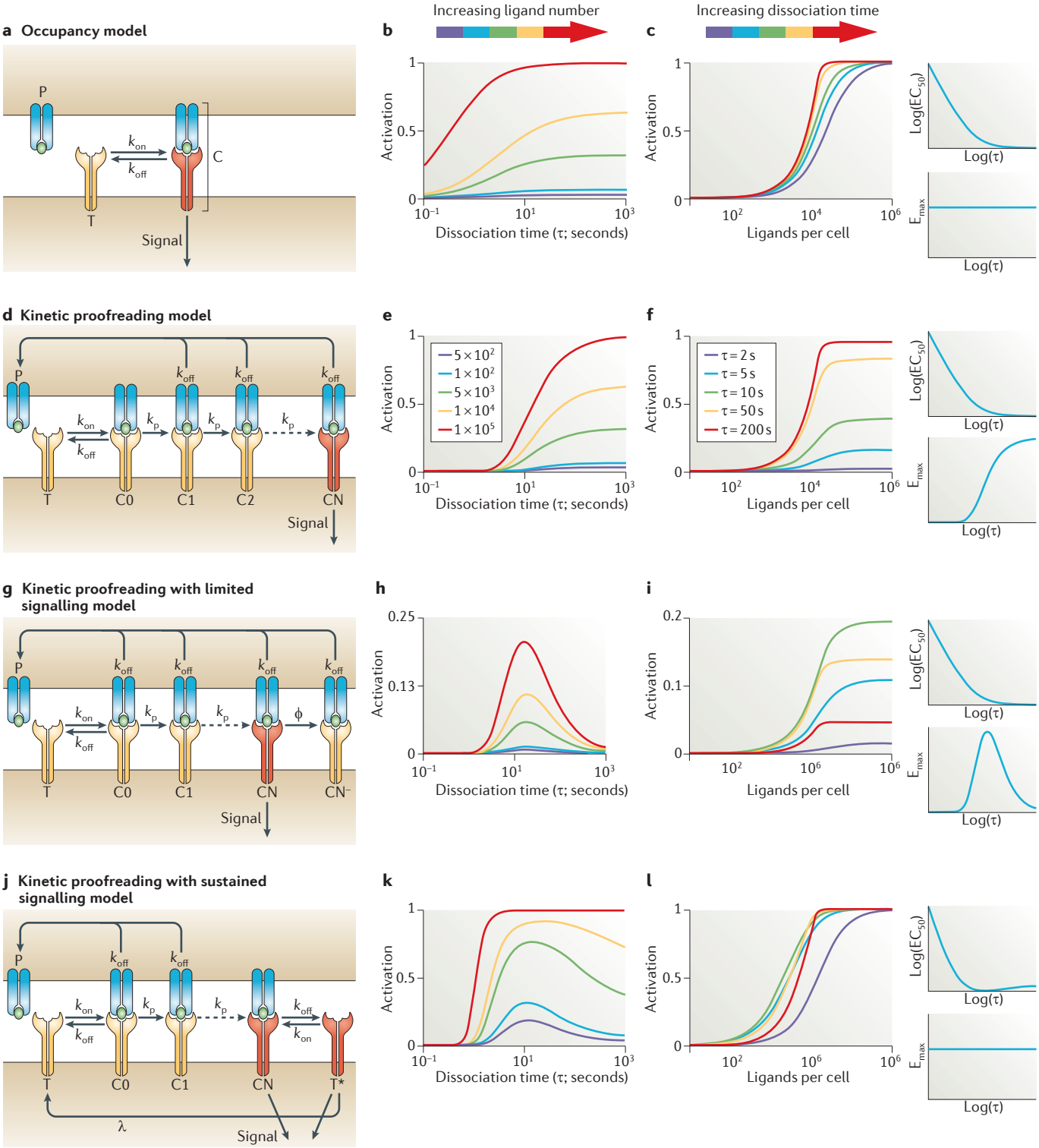

Figure 2 | **Phenotypic models of T cell activation.** For each of the model schematics (left), the predicted T cell activation over the dissociation time (centre) and over peptide–MHC (pMHC) number (right) are shown. Each model makes a qualitatively different prediction in a dose–response assay, yet differs by few reactions (or even by just one reaction). All calculations are carried out with identical on-rate (k_{on}) values and the indicated dissociation time ($\tau = 1/k_{off}$). The inverse relationship between the potency (EC_{50}) and τ translates into a direct relationship between EC_{50} and the dissociation constant (K_d), as $K_d = k_{off}/k_{on}$. In each model, free pMHC complexes (denoted 'P') can bind to free T cell receptors (TCRs; denoted 'T') to form a TCR–pMHC complex that may undergo a series of 'N' biochemical modifications (denoted as complexes C0, C1, C2 and CN) with a rate of k_p. The signalling-competent TCR state (CN) is denoted in red and differs for each model. In the limited signalling model, the signalling-competent TCR is made non-signalling (CN^-) with a rate of Φ even though the pMHC remains bound. In the sustained signalling model, signalling-competent TCRs remain in this state even after pMHC unbinding (T*) and these TCRs return to their unmodified state with a rate of λ. See Further information for the link to a website featuring animations of these models. See Supplementary information S1 for details about model formulations, calculations and parameter values, as well as a summary of the predictors of EC_{50} and E_{max}.

Experimental support for phenotypic models

In some form or another, there is experimental support for all of the proposed phenotypic models of T cell activation. Experiments have shown a correlation between EC_{50} and K_d in a number of systems[4–6,13], which is consistent with all of the proposed phenotypic models (FIG. 2). It follows that EC_{50}–K_d correlations cannot be used to discriminate between the models. By contrast, some of these experiments have shown that the maximum response depends on the pMHC binding parameters, including correlations between maximum response and dissociation time (or k_{off})[6,9,13,16]; this cannot be explained by the occupancy model nor by the kinetic proofreading with sustained signalling model, suggesting that these two models are incomplete. However, there have also been reports of an optimal dissociation time for T cell activation[7–9,11], which cannot be explained by the occupancy model or the kinetic proofreading model. Taken together, this would suggest that the only model that cannot be rejected is the kinetic proofreading with limited signalling model.

However, González *et al.*[11] carried out experiments at low and high antigen doses, and found that an optimal dissociation time disappeared at high doses. This result is inconsistent with the limited signalling model but is consistent with the sustained signalling model. We note that only this single study reports a dose-dependent optimum. Given these limited data in support of the sustained signalling model and the large datasets that are inconsistent with it[6,9,13,16], we conclude that the majority of published data support the kinetic proofreading with limited signalling model.

Evidence for an optimal dissociation time has also come from naturally occurring TCRs and *in vivo* studies[10,12,17]. Ueno *et al.*[10] studied two T cell clones isolated from a patient with HIV that recognize a viral polymerase-derived peptide and showed that the T cell bearing the higher affinity TCR exhibited impaired functional responses. By expressing the TCRs from these clones in other primary T cells, they showed that the decreased response was not related to the state of the isolated clones but was probably a generic feature of TCR signalling. In another study[12], immunization with an intermediate-affinity peptide produced the maximal immune response as measured by, for example, the number of antigen-specific responding T cells. Interestingly, *in vitro* experiments did not detect an optimum affinity. One possible explanation that could reconcile these results is that signalling was not limited *in vitro* but was *in vivo*, which may reflect a change in the T cell signalling machinery that could arise as a result of other receptor–ligand interactions.

The kinetic proofreading with limited signalling model predicts that the maximal response, but not the potency, will exhibit an optimum (FIG. 2i). This implies that the dose–response curves predicted by this model may intersect for specific dissociation times (not shown in the figure). This would mean that at a low dose, one antigen will outperform another at activating a T cell, whereas at a high dose their performance would be reversed (see figure 4 in REF 13). Although not explicitly stated, previous work suggests that dose–response curves may intersect such that the relative activity of antigens does not simply depend on their binding properties but also on the dose at which they are presented[2,6,38].

In its present formulation, the kinetic proofreading with negative feedback model is unable to reproduce an optimal dissociation time but does predict an optimal pMHC dose for T cell activation (FIG. 3). There is some experimental evidence for an optimal antigen dose[24,39,40], but additional work with antigens of varying affinities is needed.

Extensions of phenotypic models

Effect of thresholds and switch-like responses. So far, we have assumed that the fraction of signalling-competent TCRs in each model directly determines the extent of activation in individual T cells. However, TCR signals are processed by the complex cellular signalling machinery[1] (FIG. 4a,b), which ultimately determines the extent of T cell activation. Given that cellular signalling is known to exhibit thresholds and switches[23,41–43], we examine the consequences of such signal processing on phenotypic model predictions.

There is evidence for digital signalling in T cells, whereby the concentration of phosphorylated extracellular signal-regulated kinase (pERK) in individual T cells seems to exist in only two modes — namely, either fully dephosphorylated or fully phosphorylated[23,42]. Mechanisms for producing such all-or-none responses often involve feedback between signalling proteins[42,44]. Assuming that cellular signalling is an all-or-none event, it produces a 'good' threshold and a 'good' switch, and ultimately changes the predicted dose–response from phenotypic models (FIG. 4c). T cell activation is now predicted to be highly sensitive to the number of ligands, and this produces steep dose–response curves. Such highly sensitive dose–response curves have been experimentally observed for various functional T cell responses, such as the production of interleukin-2 (IL-2), tumour necrosis factor and interferon-γ (IFNγ), and certain functional readouts — such as CD69 expression — seem to occur in an all-or-none manner[6,13,42,45].

A key drawback with all-or-none cellular signalling is that it cannot explain the differential activation states of certain functional responses in individual T cells, which is further exemplified by the fact that E_{max} seems to be independent of the dissociation time (FIG. 4c). This is inconsistent with experimental data showing that the amount of IFNγ produced by individual T cells directly depends on the pMHC concentration and dissociation time[13,46], and it has recently been shown that the rate of IL-2 production is proportional to antigen dose[47].

One possible way to reconcile these observations is to assume that the cellular signalling pathway for these functional responses exhibits a threshold but not a switch (FIG. 4d). A simple signalling mechanism to produce a good threshold but a poor switch is multisite phosphorylation[48]. Under this assumption, we find that T cell activation is sensitive to ligand number while still maintaining differential activation states for individual T cells. Interestingly, experiments measuring the number of triggered TCRs (a proxy for TCR signalling) as a function of IFNγ have produced this precise relationship[41].

Digital signalling
A mode of cellular signalling whereby the concentration of a signalling protein in individual cells is confined to discrete states (for example, all protein is either fully phosphorylated or fully dephosphorylated in a cell). This is in contrast to analogue signalling, in which the concentration of a signalling protein in individual cells is found in a continuum of states.

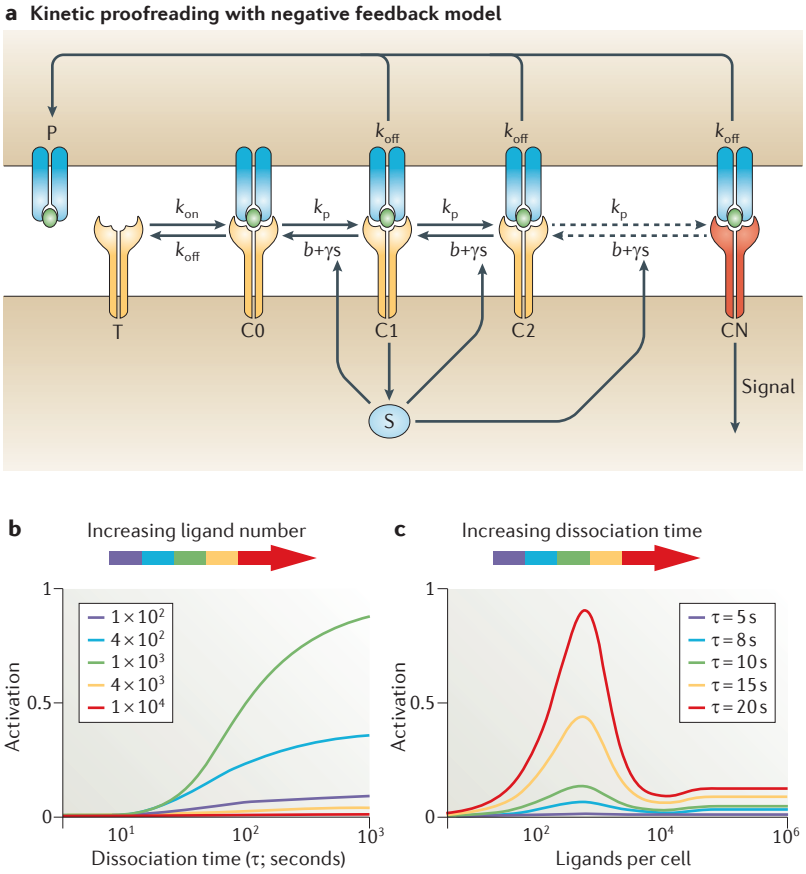

Figure 3 | **Kinetic proofreading with negative feedback model.** A schematic of the model is shown (**a**), along with the predicted T cell activation over the dissociation time (**b**) and peptide–MHC (denoted 'P') number (**c**). The T cell receptor (TCR; denoted 'T') undergoes a series of 'N' biochemical modifications (denoted as complexes C0, C1, C2 and CN) with a rate of k_p. The signalling-competent TCR state (CN) is shown in red. In this model, an intermediate state (C1) activates a cytosolic molecule — such as SH2 domain-containing protein tyrosine phosphatase 1 (SHP1; labelled 'S') — that can reverse intermediate modifications. See Supplementary information S1 for details about model formulation, calculations and parameter values.

Effect of a second pMHC ligand. Experimental work has also revealed the intriguing effects on T cell activation (induced by an agonist pMHC) that occur upon co-presentation of a second pMHC complex (FIG. 5). The presentation of a second pMHC complex can actually decrease the T cell response to an agonist, and such ligands have been termed antagonists[14,34,49–54]. These antagonist ligands are typically altered peptide ligands of the agonist that have a shorter dissociation time[51,53,54]. Interestingly, self-pMHC complexes — which are expected to have shorter dissociation times than antagonists — have been suggested to act synergistically with the agonist, leading to enhanced T cell responses[55,56]. It is reasonable to assume that within the limit of very short dissociation times, the pMHC complex will no longer interact with the TCR and such null pMHC complexes are expected to have no effect on T cell activation. Collectively, this work suggests a complicated regulation of T cell activation by the presentation of multiple pMHC complexes (FIG. 5).

Altered peptide ligands (APLs). Peptides that are analogues of an original antigenic peptide. They commonly have amino acid substitutions at residues that make contact with the T cell receptor (TCR). TCR engagement by these APLs usually leads to partial or incomplete T cell activation. Some APLs (antagonists) can specifically antagonize and inhibit T cell activation by the wild-type antigenic peptide.

The precise mechanisms by which antagonist pMHC complexes decrease and self-pMHC complexes increase T cell activation are controversial. It has been reported that antagonist stimulation results in incomplete patterns of TCR ζ-chain phosphorylation and a failure to activate ZAP70 (REFS 34,49,50,52), which is consistent with a kinetic proofreading model in which antagonist binding leads to some but not all TCR modifications. Antagonists have been shown to promote the polarization of the T cell Golgi away from the adjoining dendritic cells that were presenting agonist ligands[54], which indicates that the dissociation time that is necessary for immunological synapse assembly is shorter than that needed for activation. The ability of antagonists to dominate the polarization of the TCR signalling machinery and initiate incomplete signalling raises the question of whether antagonism is mediated simply by antagonists outcompeting agonists for TCR occupancy, or if antagonists produce an inhibitory signal. The question has been investigated in experiments involving T cell hybridomas that express two independent TCRs to determine whether the stimulatory activity of an agonist pMHC complex that binds one TCR can be reduced by an antagonist pMHC complex that binds the other TCR. In this system, some investigators did not find evidence for cross-antagonism[57,58], whereas others did[59,60]. It has been argued that a reason for the discrepant results could be that the expression level and spatial separation of the TCRs mean that a local inhibitory signal from one TCR may not affect the other[61]. There is no clear consensus on the precise mechanism of antagonism, but signalling-dependent theories have suggested that proteins could associate with the incompletely phosphorylated TCR ζ-chains through single SRC homology 2 (SH2) domains[49,61]. These proteins would be displaced during full T cell activation by ZAP70, which has a stronger interaction with fully phosphorylated immunoreceptor tyrosine-based activation motifs through its tandem SH2 domains. In agreement with this, the cytoplasmic tyrosine phosphatase SHP1 was found to be associated with both TCRs during a dual TCR experiment that showed cross-antagonism[59].

The effect of a second pMHC complex (presented at 3,000 ligands per cell) on T cell activation for all phenotypic models is shown in FIG. 6. We find that only the kinetic proofreading with negative feedback model predicts the possibility of antagonism as a result of the initiation of negative feedback, which inhibits the response to the agonist. Antagonism is observed for the kinetic proofreading and the kinetic proofreading with limited signalling models at very high concentrations of the second pMHC complex, but the decreased response in this case is mediated by the antagonist ligand outcompeting the agonist for TCR occupancy (see Supplementary information S1 (page 15)). As discussed above, experimental data on antagonism are controversial and in many studies, a very high concentration of the antagonistic pMHC complex is required to observe inhibition. This means that it is difficult to reject a model on the basis of whether or not it exhibits antagonism. Note that none of the current phenotypic models are able to reproduce the qualitative observation of co-presentation (FIG. 5).

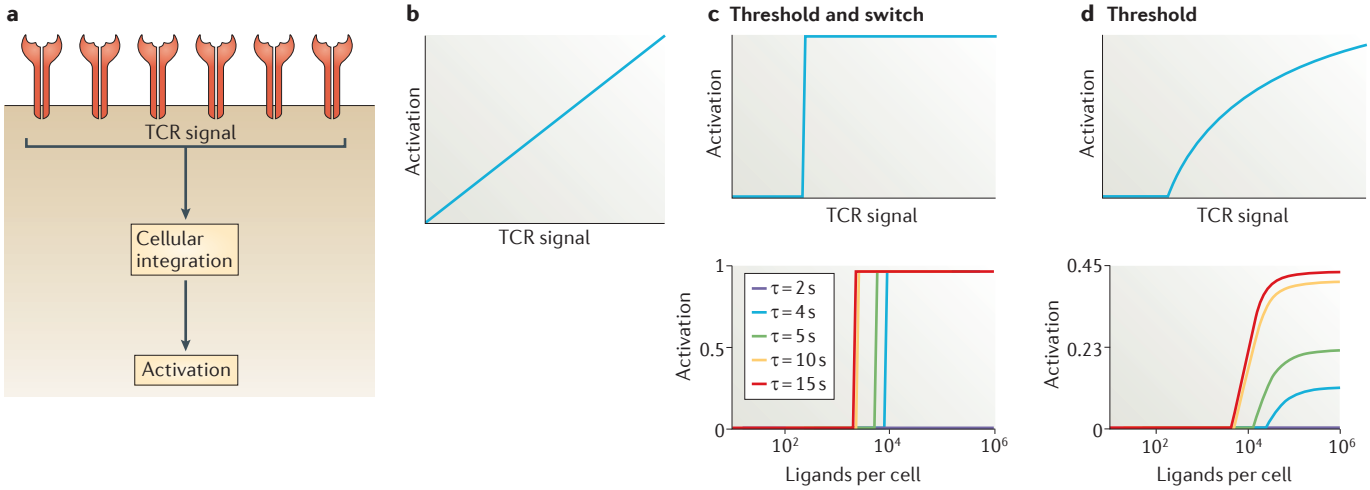

Figure 4 | **Effects of thresholds and switches in cellular signalling on T cell activation.** The cellular signalling machinery integrates signals from signalling-competent T cell receptors (TCRs) and 'translates' this information into the degree of T cell activation (**a**). All models that have been presented so far have assumed that the cellular signalling machinery linearly relates the TCR signal into T cell activation (**b**). The predicted T cell activation of kinetic proofreading with limited signalling is shown for a setting in which the cellular signalling machinery produces good thresholds and switches (**c**) — for example, digital signalling — and for an example in which there are good thresholds and poor switches (**d**). Similar results are found with other phenotypic models (see Supplementary information S1 (page 14)).

Effect of co-receptors. The effect of co-receptors on the relationship between the TCR–pMHC binding parameters and T cell activation has also been investigated. A study by Holler & Kranz[4] showed that CD8 generally increased the pMHC complex potency (reduced the EC_{50}). At the extremes, high-affinity pMHC complexes were found to be sufficiently stimulatory without CD8, and pMHC complexes with low affinities (K_d > 3 μM) require CD8 in order to stimulate T cells[4,62]. These effects are not a result of cooperative binding, as it has been shown that the binding of TCR and co-receptors to pMHC complexes are independent[63,64]. Instead, it is likely that co-receptors increase T cell sensitivity by facilitating the formation of a ternary TCR–pMHC–co-receptor complex, which is stabilized by an interaction between the TCR and co-receptor through LCK and/or ZAP70 (REFS 65,66); this is consistent with structural data[67]. Co-receptors have been found to modulate the properties of ligands that on their own do not produce a T cell response. Such ligands can act as antagonists when presented to cells that lack CD8, but can act as co-agonists in the presence of CD8 (REF. 14). This is thought to be caused by the recruitment of CD8 to the immunological synapse in a peptide-independent but MHC-dependent manner[56]. Similar results have been found for CD4 (REF. 52). In addition to modulating the effective TCR–pMHC kinetics, co-receptors — by virtue of their association with LCK — may also alter the rate of kinetic proofreading.

The formation of a ternary complex coupled to the modification of kinetic proofreading introduces a large number of unknowns, which may explain why the implementation of co-receptors has differed between mathematical models[28,68–70]. Additional work is needed to independently determine the contribution of co-receptors to modulating the TCR–pMHC binding kinetics and to altering the kinetic proofreading process before accurate predictions can be made.

Application to T cell differentiation. Signalling downstream of the TCR following antigenic stimulation has also been implicated in T cell differentiation. In the case of $CD4^+$ T cells, it is generally accepted that a unique cytokine profile will determine their differentiation into several different T helper (T_H) cell lineages[71] (for example, IFNγ- and IL-12-producing T_H1 cells, and IL-4-producing T_H2 cells) in response to the same antigenic stimulation. However, studies have also shown that the dose of antigen can influence T cell differentiation both *in vitro*[72–74] and *in vivo*[75], with high and low antigen doses producing T_H1 cells and T_H2 cells, respectively. Given that TCR signalling is determined by both antigen dose and the TCR–pMHC binding parameters (FIG. 2), it is no surprise that the TCR–pMHC binding kinetics may also influence differentiation, with low-affinity ligands favouring a T_H2 cell response[76,77]. Low-dose antigenic stimulation has also been shown to favour the induction of regulatory T cells[78,79].

It is interesting to consider how phenotypic models of T cell activation — which directly predict the TCR signal — can be modified or directly applied to the study of T cell differentiation. The kinetic proofreading with limited signalling model, for example, would suggest that pMHC complexes with both short and long dissociation times (affinities) will result in T_H2 cell differentiation, whereas T_H1 cell differentiation will exhibit an optimum as a function of dissociation time. The kinetic proofreading with negative feedback model would predict that both low and high doses of antigen can induce

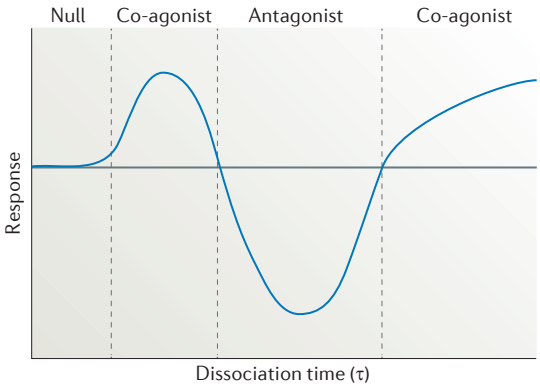

Figure 5 | **Modulation of T cell activation by co-presentation of a second peptide–MHC complex.** The presentation of an agonist peptide–MHC (pMHC) is known to elicit T cell responses (horizontal grey line). However, the co-presentation of a second pMHC is known to modulate this response (blue line) and this modulation depends on the dissociation time of the second pMHC (x-axis). Co-agonist and antagonist effects may be induced by self-pMHC, altered self-pMHC (for example, in cancer) and foreign pMHC. Presently, no model of T cell activation can reproduce these results.

T_H2 cell differentiation, which has been experimentally observed[72]. We note that it is unclear what information the TCR–pMHC dissociation time provides to the immune system that would make it beneficial to mount a T_H1-type versus T_H2-type immune response. The present analysis highlights that coupling differentiation experiments with the titration of pMHC complexes of varying affinities can be used to infer phenotypic models of differentiation.

Effect of two-dimensional interactions. The development of T cell activation models has relied almost exclusively on relating functional T cell responses to TCR–pMHC binding parameters that are determined when at least one of the proteins is in solution (for example, surface plasmon resonance-based measurements). However, the TCR and pMHC are confined to membranes and — similar to many other receptor–ligand interactions — they interact at the interface between two cells. The relationship between the membrane (or two-dimensional (2D)) binding parameters and the solution (or three-dimensional (3D)) binding parameters remains controversial. To develop models of T cell activation, it has been implicitly assumed that the measured 3D binding parameters are linearly related to the 2D binding parameters. In the following sections, we discuss two processes that may affect this assumption.

Rebinding may influence 2D dissociation times. Bimolecular reactions between proteins that are confined to the plasma membrane are thought to be limited by diffusion because the membrane diffusion coefficient is small (generally $<1\ \mu m^2/s^{-1}$). This means that upon unbinding, proteins that are confined to membranes can have a high probability of rebinding (instead of diffusing apart) and this process is predicted to be rapid (occurring within submilliseconds). Given that rebinding has been theoretically predicted[80] and experimentally observed[81] for cytosolic proteins, it is expected to be even more pronounced when both proteins are confined to membranes.

The implication of this for the TCR is that intervals between rebinding events may not be detected and therefore the effective 2D dissociation time is approximately equal to the 3D dissociation time multiplied by the number of rebinding events[15,82,83]. As the number of rebinding events is determined, in part, by the on-rate (k_{on}), the 2D dissociation time may exhibit a dependency on k_{on}. Although direct evidence for TCR–pMHC rebinding has not been reported, the rebinding-corrected 2D dissociation time has been shown to be a better predictor of T cell activation than the 3D dissociation time[13,15,83].

It is worth noting that rebinding can also be enhanced by the clustering of TCRs, membrane alignment and conformational changes in the TCR. Recently, induced rebinding has been proposed to improve antigen discrimination[84].

Force may influence 2D dissociation times. Multiple processes have been proposed to impart tension on the TCR–pMHC complex at the T cell–APC interface. Highly abundant long (≈50 nm) surface molecules — such as CD45, CD148 and CD43 — are predicted to indirectly produce tension on short (≈13 nm) TCR–pMHC interactions, and a mechanical model has predicted this tension to be in the range of 10 pN[85]. Other cytoskeleton-driven sources of force include the relative movements of cell membranes and the lateral transport of cell-surface molecules within the membrane[86].

Precisely how the dissociation time of TCR–pMHC interactions will depend on force remains an open question. A study using a flow chamber assay reports that nearly all interactions subjected to a force exhibit shorter dissociation times that are characteristic of slip bonds[87]. It is worth noting that a single pMHC exhibited longer dissociation times under force, which is characteristic of catch bonds (for example, some integrins are known to form catch bonds[88]). A recent study by Zhu and colleagues[89] found that agonists for the OT-I TCR exhibited catch-bond behaviour using the biomembrane force probe assay.

The significance of catch bonds is that the 3D dissociation time (measured without an applied force) may not exhibit a positive correlation with the 2D dissociation time (measured with an applied force). Future work is needed to determine whether these results can be generalized to other TCRs. We speculate that all categories of pMHC ligands (for example, agonists, antagonists and ligands that have no functional effect) may exhibit catch-bond behaviour but that ultimately, the effective 2D dissociation time will determine the functional T cell response.

Direct measurements of 2D binding parameters. Measurements of 2D binding parameters at cell interfaces are challenging. Published studies have used a fluorescence resonance energy transfer (FRET)-based[90] and an

On-rate
(k_{on}). The rate constant of T cell receptor–peptide–MHC binding (with typical units of $\mu M^{-1}s^{-1}$ for three-dimensional solution measurements and typical units of μm^2s^{-1} for two-dimensional membrane measurements).

Slip bonds
Molecular bonds for which the dissociation time decreases under tension.

Catch bonds
Molecular bonds for which the dissociation time increases under tension.

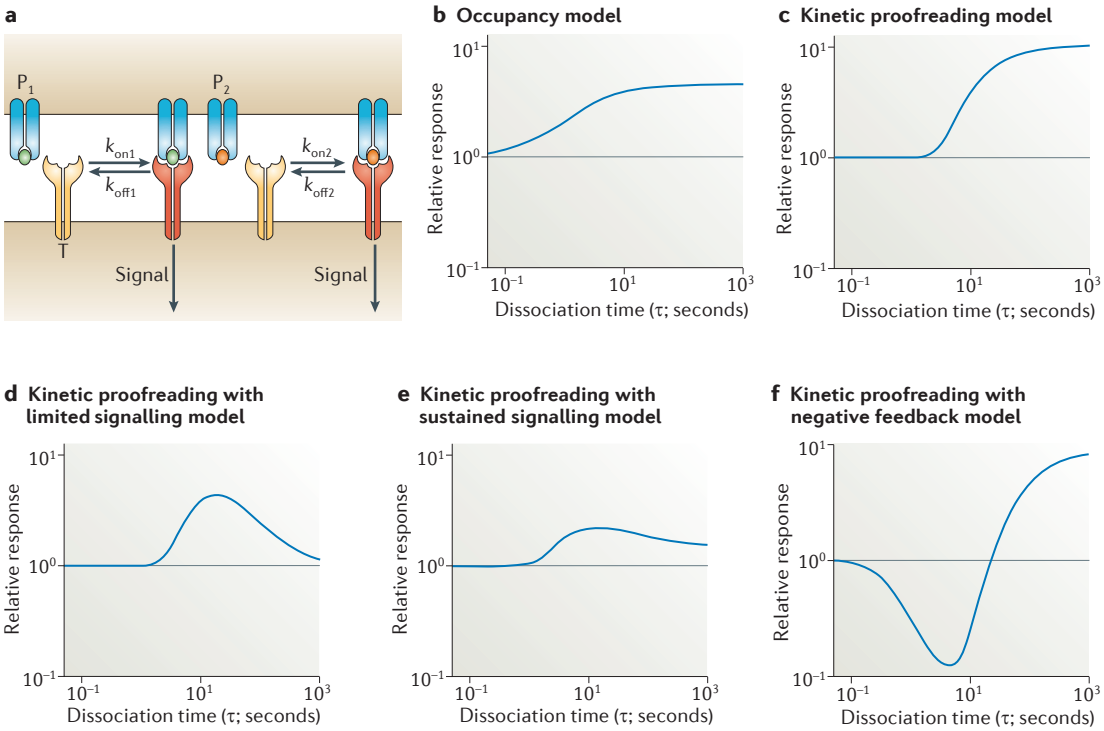

Figure 6 | **Co-presentation of a second pMHC is predicted to inhibit T cell activation in the kinetic proofreading with negative feedback model.** A schematic of the binding reactions when two peptide–MHC (pMHC; denoted 'P') complexes are present (**a**). Panels **b–f** show the fold change in T cell activation when the second pMHC (P_2) is presented at 3,000 ligands per cell with the indicated dissociation time (x-axis). The first pMHC (P_1) is assumed to have a dissociation time of 10 s and be presented at 1,000 ligands per cell. See Supplementary information S1 (page 15) for a figure showing the effects of changing the concentration of the second pMHC. T, T cell receptor.

adhesion-based[91] assay to examine 2D binding parameters. Both studies report that the 2D dissociation time is shorter than the 3D dissociation time, which is consistent with the slip bonds under tension. In support of this, inhibitors of the actin cytoskeleton increase the 2D dissociation time[90]. More recently, a study using indirect single-particle tracking-based assays to measure 2D binding parameters reported no changes between the 3D and 2D dissociation times[92]. This conclusion is consistent with slip bonds under tension, combined with rebinding.

All mathematical models of T cell activation require 2D TCR–pMHC binding parameters. It follows that the incorporation of rebinding and/or force into these models involves transforming the 3D binding parameters into 2D binding parameters, or directly measuring the 2D binding parameters. It is important to note that correlations between 3D binding parameters (without an applied force) and the functional T cell response have been very high, and therefore it is likely that the relationships between the 3D and 2D binding parameters are monotonically increasing.

Conclusion

In this Analysis article, we have reformulated models of T cell activation into simple phenotypic models (BOX 1), which has allowed us to directly compare the predicted T cell response for pMHC complexes at different concentrations and binding parameters. We have found that the phenotypic model that is most compatible with experimental data is the kinetic proofreading with limited signalling model. However, we emphasize that the published data are incomplete, with experiments typically using only a small panel of TCRs (or pMHC complexes) with a limited range of affinities, and a single or just a few different doses of antigen or pMHC. The study of pMHC co-presentation, co-receptors, differentiation, and other costimulatory or co-inhibitory molecules is often limited to qualitative studies involving pMHC ligands that have an unknown affinity and a fixed concentration. Phenotypic models of T cell activation can be used to guide the design of modified TCRs and chimeric antigen receptors for adoptive T cell-based therapies[93–95]. We note that all of the phenotypic models that we have considered make no explicit assumptions about the mechanism by which pMHC binding generates intracellular signalling — a process termed TCR triggering — and these phenotypic models are largely consistent with all known mechanisms of TCR triggering[96]. This Analysis article highlights that detailed dose–response experiments using many TCR–pMHC pairs with a wide range of affinities can be used to dramatically constrain, reject and formulate models of T cell activation.

1. Smith-Garvin, J. E., Koretzky, G. a. & Jordan, M. S. T cell activation. *Annu. Rev. Immunol.* **27**, 591–619 (2009).
2. Andersen, P. S., Geisler, C., Buus, S., Mariuzza, R. A. & Karjalainen, K. Role of the T cell receptor ligand affinity in T cell activation by bacterial superantigens. *J. Biol. Chem.* **276**, 33452–33457 (2001).
3. Krogsgaard, M., Prado, N., Adams, E. & He, X.-l. Evidence that structural rearrangements and/or flexibility during TCR binding can contribute to T cell activation. *Mol. Cell* **12**, 1367–1378 (2003).
4. Holler, P. D. & Kranz, D. M. Quantitative analysis of the contribution of TCR/pepMHC affinity and CD8 to T cell activation. *Immunity* **18**, 255–264 (2003).
5. Tian, S., Maile, R., Collins, E. & Frelinger, J. $CD8^+$ T cell activation is governed by TCR-peptide/MHC affinity, not dissociation rate. *J. Immunol.* **179**, 2952–2960 (2007).
6. Chervin, A. S. *et al.* The impact of TCR-binding properties and antigen presentation format on T cell responsiveness. *J. Immunol.* **183**, 1166–1178 (2009).
7. Kalergis, A. M. *et al.* Efficient T cell activation requires an optimal dwell-time of interaction between the TCR and the pMHC complex. *Nature Immunol.* **2**, 229–234 (2001).
This is the first study to provide experimental evidence in support of an optimal dissociation time for T cell activation.
8. Coombs, D., Kalergis, A. M., Nathenson, S. G., Wofsy, C. & Goldstein, B. Activated TCRs remain marked for internalization after dissociation from pMHC. *Nature Immunol.* **3**, 926–931 (2002).
9. Irving, M. *et al.* Interplay between T cell receptor binding kinetics and the level of cognate peptide presented by major histocompatibility complexes governs $CD8^+$ T cell responsiveness. *J. Biol. Chem.* **287**, 23068–23078 (2012).
10. Ueno, T., Tomiyama, H., Fujiwara, M., Oka, S. & Takiguchi, M. Functionally impaired HIV-specific CD8 T cells show high affinity TCR-ligand interactions. *J. Immunol.* **173**, 5451–5457 (2004).
11. González, P. A. *et al.* T cell receptor binding kinetics required for T cell activation depend on the density of cognate ligand on the antigen-presenting cell. *Proc. Natl Acad. Sci. USA* **102**, 4824–4829 (2005).
This study provided the only known experimental evidence for a concentration-dependent optimum and constructed a modified kinetic proofreading model that can explain this result.
12. Corse, E., Gottschalk, R. A., Krogsgaard, M. & Allison, J. P. Attenuated T cell responses to a high-potency ligand *in vivo*. *PLoS Biol.* **8**, 1–12 (2010).
13. Dushek, O. *et al.* Antigen potency and maximal efficacy reveal a mechanism of efficient T cell activation. *Sci. Signal.* **4**, ra39 (2011).
This study resolved the long-standing debate between occupancy-based and kinetic proofreading-based models by showing that the maximal response depends on the dissociation time at the cell population and single-cell level.
14. Stone, J. D. *et al.* Opposite effects of endogenous peptide–MHC class I on T cell activity in the presence and absence of CD8. *J. Immunol.* **186**, 5193–5200 (2011).
15. Govern, C. C., Paczosa, M. K., Chakraborty, A. K. & Huseby, E. S. Fast on-rates allow short dwell time ligands to activate T cells. *Proc. Natl Acad. Sci. USA* **107**, 8724–8729 (2010).
16. Zhong, S. *et al.* T-cell receptor affinity and avidity defines antitumor response and autoimmunity in T-cell immunotherapy. *Proc. Natl Acad. Sci. USA* **110**, 6973–6978 (2013).
17. McMahan, R. H. *et al.* Relating TCR-peptide-MHC affinity to immunogenicity for the design of tumor vaccines. *J. Clin. Invest.* **116**, 2543–2551 (2006).
18. McKeithan, T. W. Kinetic proofreading in T-cell receptor signal transduction. *Proc. Natl Acad. Sci. USA* **92**, 5042–5046 (1995).
This paper describes the first application of kinetic proofreading to TCR signalling, which has formed the basis for all models of T cell signalling and activation.
19. Valitutti, S. & Lanzavecchia, A. Serial triggering of TCRs: a basis for the sensitivity and specificity of antigen recognition. *Immunol. Today* **18**, 299–304 (1997).
This is the first study to propose that a trade-off between serial binding and kinetic proofreading will produce an optimal dissociation time for T cell activation.
20. Andersen, P. S., Menné, C., Mariuzza, R. A., Geisler, C. & Karjalainen, K. A response calculus for immobilized T cell receptor ligands. *J. Biol. Chem.* **276**, 49125–49132 (2001).
21. Chan, C., George, A. J. & Stark, J. Cooperative enhancement of specificity in a lattice of T cell receptors. *Proc. Natl Acad. Sci. USA* **98**, 5758–5763 (2001).
22. Van Den Berg, H. A., Burroughs, N. J. & Rand, D. A. Quantifying the strength of ligand antagonism in TCR triggering. *Bull. Math. Biol.* **64**, 781–808 (2002).
23. Altan-Bonnet, G. & Germain, R. N. Modeling T cell antigen discrimination based on feedback control of digital ERK responses. *PLoS Biol.* **3**, e356 (2005).
This paper modified the kinetic proofreading model to include both positive and negative feedback, which improved antigen discrimination and the ability to predict a bimodal (digital) ERK response.
24. Francois, P., Voisinne, G., Siggia, E. D., Altan-Bonnet, G. & Vergassola, M. Phenotypic model for early T-cell activation displaying sensitivity, specificity, and antagonism. *Proc. Natl Acad. Sci. USA* **110**, E888–E897 (2013).
This paper formulated a simple phenotypic model of kinetic proofreading with a single negative feedback that exhibits improved antigen discrimination and predicts an optimum in the dose–response curve.
25. Wofsy, C., Coombs, D. & Goldstein, B. Calculations show substantial serial engagement of T cell receptors. *Biophys. J.* **80**, 606–612 (2001).
26. Van Den Berg, H. A., Rand, D. A. & Burroughs, N. J. A reliable and safe T cell repertoire based on low-affinity T cell receptors. *J. Theor. Biol.* **209**, 465–486 (2001).
27. Burroughs, N. J., Lazic, Z. & van der Merwe, P. A. Ligand detection and discrimination by spatial relocalization: A kinase-phosphatase segregation model of TCR activation. *Biophys. J.* **91**, 1619–1629 (2006).
28. Dushek, O. & Coombs, D. Analysis of serial engagement and peptide-MHC transport in T cell receptor microclusters. *Biophys. J.* **94**, 3447–3460 (2008).
29. Varma, R., Campi, G., Yokosuka, T., Saito, T. & Dustin, M. L. T cell receptor-proximal signals are sustained in peripheral microclusters and terminated in the central supramolecular activation cluster. *Immunity* **25**, 117–127 (2006).
30. Lee, K. H. *et al.* The immunological synapse balances T cell receptor signaling and degradation. *Science* **302**, 1218–1222 (2003).
31. Valitutti, S., Muller, S. & Cella, M. Serial triggering of many T-cell receptors by a few peptide MHC complexes. *Nature* **375**, 148–151 (1995).
32. Martinez-Martin, N. *et al.* T cell receptor internalization from the immunological synapse is mediated by TC21 and RhoG GTPase-dependent phagocytosis. *Immunity* **35**, 208–222 (2011).
33. Choudhuri, K. *et al.* Polarized release of T-cell-receptor-enriched microvesicles at the immunological synapse. *Nature* **507**, 118–123 (2014).
34. Stefanová, I. *et al.* TCR ligand discrimination is enforced by competing ERK positive and SHP-1 negative feedback pathways. *Nature Immunol.* **4**, 248–254 (2003).
This study provides mechanistic evidence for a SHP1-mediated negative feedback and an ERK-mediated positive feedback.
35. Li, Q.-J. *et al.* miR-181a is an intrinsic modulator of T cell sensitivity and selection. *Cell* **129**, 147–161 (2007).
36. Wylie, D. C., Das, J. & Chakraborty, A. K. Sensitivity of T cells to antigen and antagonism emerges from differential regulation of the same molecular signaling module. *Proc. Natl Acad. Sci. USA* **104**, 5533–5538 (2007).
37. Lipniacki, T., Hat, B., Faeder, J. R. & Hlavacek, W. S. Stochastic effects and bistability in T cell receptor signaling. *J. Theor. Biol.* **254**, 110–122 (2008).
38. Zhao, Y. *et al.* High-affinity TCRs generated by phage display provide $CD4^+$ T cells with the ability to recognize and kill tumor cell lines. *J. Immunol.* **179**, 5845–5854 (2011).
39. Wolchinsky, R. *et al.* Antigen-dependent integration of opposing proximal TCR-signaling cascades determines the functional fate of T lymphocytes. *J. immunol.* **192**, 2109–2119 (2014).
40. Chiu, Y. *et al.* Sprouty-2 regulates HIV-specific T cell polyfunctionality. *J. Clin. Invest.* **124**, 198–208 (2014).
41. Viola, A. & Lanzavecchia, A. T cell activation determined by T cell receptor number and tunable thresholds. *Science* **273**, 104–106 (1996).
This study provides evidence that IFNγ exhibits a good threshold but a poor switch to proximal TCR signalling.
42. Das, J. *et al.* Digital signaling and hysteresis characterize ras activation in lymphoid cells. *Cell* **136**, 337–351 (2009).
43. van den Berg, H. A. *et al.* Cellular-level versus receptor-level response threshold hierarchies in T-cell activation. *Front. Immunol.* **4**, 250 (2013).
44. Tyson, J. J., Chen, K. C. & Novak, B. Sniffers, buzzers, toggles and blinkers: dynamics of regulatory and signaling pathways in the cell. *Curr. Opin. Cell Biol.* **15**, 221–231 (2003).
45. Huang, J. *et al.* A single peptide-major histocompatibility complex ligand triggers digital cytokine secretion in $CD4^+$ T cells. *Immunity* **39**, 846–857 (2013).
46. Itoh, Y. & Germain, R. Single cell analysis reveals regulated hierarchical T cell antigen receptor signaling thresholds and intraclonal heterogeneity. *J. Exp. Med.* **186**, 757–766 (1997).
47. Tkach, K. E. *et al.* T cells translate individual, quantal activation into collective, analog cytokine responses via time-integrated feedbacks. *eLife* **3**, e01944 (2014).
48. Gunawardena, J. Multisite protein phosphorylation makes a good threshold but can be a poor switch. *Proc. Natl Acad. Sci. USA* **102**, 14617–14622 (2005).
49. Sloan-Lancaster, J., Shaw, A. S., Rothbard, J. B. & Allen, P. M. Partial T cell signaling: altered phospho-ζ and lack of zap70 recruitment in APL-induced T cell anergy. *Cell* **79**, 913–922 (1994).
50. Madrenas, J. *et al.* Zeta phosphorylation without ZAP-70 activation induced by TCR antagonists or partial agonists. *Science* **267**, 515–518 (1995).
51. Lyons, D. S. *et al.* A TCR binds to antagonist ligands with lower affinities and faster dissociation rates than to agonists. *Immunity* **5**, 53–61 (1996).
52. Madrenas, J., Chau, L. A., Smith, J., Bluestone, J. A. & Germain, R. N. The efficiency of CD4 recruitment to ligand-engaged TCR controls the agonist/partial agonist properties of peptide-MHC molecule ligands. *J. Exp. Med.* **185**, 219–229 (1997).
53. Koniaras, C., Carbone, F. R., Heath, W. R. & Lew, A. M. Inhibition of naïve class I-restricted T cells by altered peptide ligands. *Immunol. Cell Biol.* **77**, 318–323 (1999).
54. Carreño, L. J. *et al.* T-cell antagonism by short half-life pMHC ligands can be mediated by an efficient trapping of T-cell polarization toward the APC. *Proc. Natl Acad. Sci. USA* **107**, 210–215 (2010).
55. Krogsgaard, M., Juang, J. & Davis, M. M. A role for "self" in T-cell activation. *Seminars Immunol.* **19**, 236–244 (2007).
56. Yachi, P. P., Lotz, C., Ampudia, J. & Gascoigne, N. R. J. T cell activation enhancement by endogenous pMHC acts for both weak and strong agonists but varies with differentiation state. *J. Exp. Med.* **204**, 2747–2757 (2007).
57. Stotz, S. H., Bolliger, L., Carbone, F. R. & Palmer, E. T cell receptor (TCR) antagonism without a negative signal: evidence from T cell hybridomas expressing two independent TCRs. *J. Exp. Med.* **189**, 253–264 (1999).
58. Daniels, M. A., Schober, S. L., Hogquist, K. A. & Jameson, S. C. Cutting edge: a test of the dominant negative signal model for TCR antagonism. *J. Immunol.* **162**, 3761–3764 (1999).
59. Dittel, B. N., Stefanova, I. & Germain, R. N. & Janeway, C. A. Cross-antagonism of a T cell clone expressing two distinct T cell receptors. *Immunity* **11**, 289–298 (1999).
60. Robertson, J. M. & Evavold, B. D. Cutting edge: dueling TCRs: peptide antagonism of $CD4^+$ T cells with dual antigen specificities. *J. Immunol.* **163**, 1750–1754 (1999).
61. Kersh, E. N., Kersh, G. J. & Allen, P. M. Partially phosphorylated T cell receptor-ζ molecules can inhibit T cell activation. *J. Exp. Med.* **190**, 1627–1636 (1999).
62. Chervin, A. S., Stone, J. D., Bowerman, N. A. & Kranz, D. M. Cutting edge: inhibitory effects of CD4 and CD8 on T cell activation induced by high-affinity noncognate ligands. *J. Immunol.* **183**, 7639–7643 (2009).
63. Wyer, J. R. *et al.* T cell receptor and coreceptor CD8αα bind peptide-MHC independently and with distinct kinetics. *Immunity* **10**, 219–225 (1999).

64. Xiong, Y., Kern, P., Chang, H. & Reinherz, E. T cell receptor binding to a pMHCII ligand is kinetically distinct from and independent of CD4. *J. Biol. Chem.* **276**, 5659–5667 (2001).
65. Pelosi, M., Bartolo, V. D. & Mounier, V. Tyrosine 319 in the interdomain B of ZAP-70 is a binding site for the Src Homology 2 domain of Lck. *J. Biol. Chem.* **274**, 14229–14237 (1999).
66. Jiang, N. *et al.* Two-stage cooperative T cell receptor-peptide major histocompatibility complex-CD8 trimolecular interactions amplify antigen discrimination. *Immunity* **34**, 13–23 (2011).
67. Yin, Y., Wang, X. X. & Mariuzza, R. A. Crystal structure of a complete ternary complex of T-cell receptor, peptide–MHC, and CD4. *Proc. Natl Acad. Sci. USA* **109**, 5405–5410 (2012).
68. Li, Q.-J. *et al.* CD4 enhances T cell sensitivity to antigen by coordinating Lck accumulation at the immunological synapse. *Nature Immunol.* **5**, 791–799 (2004).
69. Artyomov, M. N., Lis, M., Devadas, S., Davis, M. M. & Chakraborty, A. K. CD4 and CD8 binding to MHC molecules primarily acts to enhance Lck delivery. *Proc. Natl Acad. Sci. USA* **107**, 16916–16921 (2010).
70. Szomolay, B., Williams, T., Wooldridge, L. & van den Berg, H. A. Co-receptor CD8-mediated modulation of T-cell receptor functional sensitivity and epitope recognition degeneracy. *Frontiers Immunol.* **4**, 329 (2013).
71. Zhu, J. & Paul, W. E. Peripheral CD4$^+$ T-cell differentiation regulated by networks of cytokines and transcription factors. *Immunol. Rev.* **238**, 247–262 (2010).
72. Hosken, B. N. A., Shibuya, K., Heath, A. W., Murphy, K. M. & Garra, A. O. The effect of antigen dose on CD4$^+$ T helper cell phenotype development in a T cell receptor-αβ transgenic model. *J. Exp. Med.* **182**, 20–22 (1995).
73. Constant, B. S., Pfeiffer, C., Woodard, A., Pasqualini, T. & Bottomly, K. Extent of T cell receptor ligation can determine the functional differentiation of naive CD4$^+$ T cells. *J. Exp. Med.* **182**, 1591–1596 (1995).
74. Yamane, H., Zhu, J. & Paul, W. E. Independent roles for IL-2 and GATA-3 in stimulating naive CD4$^+$ T cells to generate a Th2-inducing cytokine environment. *J. Exp. Med.* **202**, 793–804 (2005).
75. Panhuys, N. V., Klauschen, F. & Germain, R. T-cell-receptor-dependent signal intensity dominantly controls CD4 + T cell polarization *in vivo*. *Immunity* **41**, 63–74 (2014).
76. Tao, X., Grant, C., Constant, S. & Bottomly, K. Induction of IL-4-producing CD4$^+$ T cells by antigenic peptides altered for TCR binding. *J. Immunol.* **158**, 4237–4244 (1997).
77. Milner, J. D., Fazilleau, N., McHeyzer-Williams, M. & Paul, W. Cutting edge: lack of high affinity competition for peptide in polyclonal CD4$^+$ responses unmasks IL-4 production. *J. Immunol.* **184**, 6569–6573 (2010).
78. Turner, M. S., Kane, L. P. & Morel, P. A. Dominant role of antigen dose in CD4$^+$ Foxp3$^+$ regulatory T cell induction and expansion. *J. Immunol.* **183**, 4895–4903 (2009).
79. Gottschalk, R. A., Corse, E. & Allison, J. P. TCR ligand density and affinity determine peripheral induction of Foxp3 *in vivo*. *J. Exp. Med.* **207**, 1701–1711 (2010).
80. Takahashi, K., Tanase-Nicola, S. & ten Wolde, P. R. Spatio-temporal correlations can drastically change the response of a MAPK pathway. *Proc. Natl Acad. Sci. USA* **107**, 2473–2478 (2010).
81. Oh, D. *et al.* Fast rebinding increases dwell time of Src homology 2 (SH2)-containing proteins near the plasma membrane. *Proc. Natl Acad. Sci. USA* **109**, 14024–14029 (2012).
82. Dushek, O., Das, R. & Coombs, D. A role for rebinding in rapid and reliable T cell responses to antigen. *PLoS Computat. Biol.* **5**, e1000578 (2009).
83. Aleksic, M. *et al.* Dependence of T cell antigen recognition on T cell receptor-peptide MHC confinement time. *Immunity* **32**, 163–174 (2010).
84. Dushek, O. & van der Merwe, P. A. An induced rebinding model of antigen discrimination. *Trends Immunol.* **35**, 153–158 (2014).
85. Allard, J. F., Dushek, O., Coombs, D. & van der Merwe, P. A. Mechanical modulation of receptor-ligand interactions at cell-cell interfaces. *Biophys. J.* **102**, 1265–1273 (2012).
86. Dustin, M. L. & Depoil, D. New insights into the T cell synapse from single molecule techniques. *Nature Rev. Immunology* **11**, 672–684 (2011).
87. Robert, P. *et al.* Kinetics and mechanics of two-dimensional interactions between T cell receptors and different activating ligands. *Biophys. J.* **102**, 248–257 (2012).
88. Zhu, C. & Chen, W. in *Single-Molecule Studies of Proteins* (ed. Oberhauser, A. F.) 235–268 (Springer, 2013).
89. Liu, B., Chen, W., Evavold, B. D. & Zhu, C. Accumulation of dynamic catch bonds between TCR and agonist peptide-MHC triggers T cell signaling. *Cell* **157**, 357–368 (2014).
90. Huppa, J. B. *et al.* TCR–peptide–MHC interactions *in situ* show accelerated kinetics and increased affinity. *Nature* **463**, 963–967 (2010).
91. Huang, J. *et al.* The kinetics of two-dimensional TCR and pMHC interactions determine T-cell responsiveness. *Nature* **464**, 932–936 (2010). **References 90 and 91 report direct measurements of the physiological TCR–pMHC kinetics at 2D membrane interfaces, showing shorter dissociation times than 3D solution measurements.**
92. O'Donoghue, G. P., Pielak, R. M., Smoligovets, A. A., Lin, J. J. & Groves, J. T. Direct single molecule measurement of TCR triggering by agonist pMHC in living primary T cells. *eLife* **2**, e00778 (2013).
93. Sadelain, M. & Brentjens, R. The promise and potential pitfalls of chimeric antigen receptors. *Curr. Opin. Immunol.* **21**, 215–223 (2009).
94. Porter, D. L., Levine, B. L., Kalos, M., Bagg, A. & June, C. H. Chimeric antigen receptor-modified T cells in chronic lymphoid leukemia. *New Engl. J. Med.* **365**, 725–733 (2011).
95. Restifo, N. P., Dudley, M. E. & Rosenberg, S. A. Adoptive immunotherapy for cancer: harnessing the T cell response. *Nature Rev. Immunol.* **12**, 269–281 (2012).
96. van der Merwe, P. A. & Dushek, O. Mechanisms for T cell receptor triggering. *Nature Rev. Immunol.* **11**, 47–55 (2011).
97. Gunawardena, J. Models in biology: 'accurate descriptions of our pathetic thinking'. *BMC Biology* **12**, 29 (2014).

Acknowledgements

M.L. is supported by a Doctoral Training Centre Systems Biology studentship from the Engineering and Physical Sciences Research Council (EPSRC). O.D. is supported by a Sir Henry Dale Fellowship that is jointly funded by the Wellcome Trust and the Royal Society (grant number 098363). This work was funded in part by Cancer Research UK (C19634/A12336).

Competing interests statement

The authors declare no competing interests.

FURTHER INFORMATION

Animations of phenotypic models: http://dushek.path.ox.ac.uk/publications

SUPPLEMENTARY INFORMATION

See online article: S1

ALL LINKS ARE ACTIVE IN THE ONLINE PDF

Supplementary Information: Phenotypic models of T cell activation

Melissa Lever[†], Philip K. Maini[‡], P. Anton van der Merwe[†], Omer Dushek[†,‡,¶]

[†]Sir William Dunn School of Pathology, University of Oxford, Oxford, Oxfordshire, United Kingdom
[‡]Wolfson Centre for Mathematical Biology, Mathematical Institute, University of Oxford, Oxford, Oxfordshire, United Kingdom
[¶]Corresponding author

Contents

1 Generation and parameter values for main text figures

1.1 Figure 2

The occupancy, kinetic proofreading, limited signalling and sustained signalling models were calculated using the analytical results derived in the next section. The dose-response plots and plots showing activation as a function of τ were normalised by T_T, so that activation was in the range $[0,\ 1]$. Parameters: number of TCRs $T_T = 1.5708 \times 10^4$, $k_{\text{on}} = 3.1831 \times 10^{-5}$ s^{-1} , $k_{\text{p}} = 1$ s^{-1}, $N = 10$, $\phi = 0.09$ s^{-1}, λ = 0.001 s^{-1}.

1.2 Figure 3

The negative feedback model is calculated as described by Francois et al (1). The dose-repsonse plot and the plot showing activation as a function of τ were calculated using the Matlab (Mathworks, MA) function *ode15s*. The plots were normalised by the most stimulating ligand in the plot, to give activation in the range of [0, 1]. Parameters: number of TCRs $T_T = 3 \times 10^4$, $S_T = 6 \times 10^5$, $k_{\text{on}} = 1 \times 10^{-4}$ s^{-1}, $N = 10$, $k_{\text{p}} = 0.252$ s^{-1}, $b = 0.04\ s^{-1}$, $\gamma = 4.4 \times 10^{-4}$.

1.3 Figure 4

The kinetic proofreading with limited signalling was calculated for the shown dissociation times and then a transformation of either 4 c) a threshold and switch or 4 d) threshold was applied to the TCR signal and the resultant activation plotted as a function of ligand dose. Parameters: number of TCRs $T_T = 1.5708 \times 10^4$, $k_{\text{on}} = 3.1831 \times 10^{-5}$ s^{-1} , $k_{\text{p}} = 1$ s^{-1}, $N = 10$, $\phi = 0.09$ s^{-1}.

1.4 Figure 6

The relative change in activation when a second ligand is co-presented compared to the first ligand alone was calculated for the occupancy, kinetic proofreading, limited signalling and sustained signalling models analytically using the results from the derivations in the next section. The negative feedback model was numerically calculated using the Matlab (Mathworks, MA) function *ode15s*. The first ligand has τ = 10 s and is presented at 10^3 ligands per cell. The second ligand has a dissociation time and ligand number denoted by the axes and is presented at 3×10^3 ligands per cell. Parameters for the occupancy, kinetic proofreading, kinetic proofreading with limited and sustained signaling: number of TCRs $T_T = 1.5708 \times 10^4$, $k_{\text{on}} = 3.1831 \times 10^{-5}$ s^{-1} , $k_{\text{p}} = 1$ s^{-1}, $N = 10$, $\phi = 0.09$ s^{-1}, λ = 0.001 s^{-1}. Parameters for the negative feedback model: number of TCRs $T_T = 3 \times 10^4$, $S_T = 6 \times 10^5$, $k_{\text{on}} = 1 \times 10^{-4}$s^{-1}, $k_{\text{p}} = 0.252$s^{-1}, $N = 10$, $b = 0.04$s^{-1}, $\gamma = 4.4 \times 10^{-4}$.

1.5 Figure S1

The effect of thresholds and switches was found for the occupancy, kinetic proofreading and sustained signalling models by calculating the models at the shown dissociation times and then applying a transformation of either c) a threshold and switch or d) a threshold to the TCR signal and the resultant activation plotted as a function of ligand dose. Parameters: number of TCRs $T_T = 1.5708 \times 10^4$, $k_{\text{on}} = 3.1831 \times 10^{-5}$ s^{-1} , $k_{\text{p}} = 1$ s^{-1}, $N = 10$, $\phi = 0.09$ s^{-1}, λ = 0.001 s^{-1}.

1.6 Figure S2

a) - e) These plots show the change in the level of T cell activation when a second ligand is co-presented compared to the first ligand alone. The first ligand has τ = 10 s and is presented at 10^3 ligands. The second

ligand has a dissociation time and ligand number denoted by the axes. The occupancy, kinetic proofreading, limited signalling and sustained signalling models were all calculated analytically using the results from the derivations in the next section. The negative feedback model was numerically calculated using the Matlab (Mathworks, MA) function *ode15s*. A heat map was applied to the matrices that contained the relative change in activation when the second ligand was co-presented. The same colorbar was used for all plots so that the models could be directly compared. Parameters for the occupancy, kinetic proofreading, kinetic proofreading with limited and sustained signaling: number of TCRs $T_T = 1.5708 \times 10^4$, $k_{\text{on}} = 3.1831 \times 10^{-5}$ s^{-1} , $k_{\text{p}} = 1$ s^{-1}, $N = 10$, $\phi = 0.09$ s^{-1}, λ = 0.001 s^{-1}. Parameters for the negative feedback model: number of TCRs $T_T = 3 \times 10^4$, $S_T = 6 \times 10^5$, $k_{\text{on}} = 1 \times 10^{-4}$s^{-1}, $k_{\text{p}} = 0.252$s^{-1}, $N = 10$, $b = 0.04$s^{-1}, $\gamma = 4.4 \times 10^{-4}$.

f) The percentage of TCR occupied by the second ligand was calculated using the analytical result for co-presentation under the occupation model, which is in the next section. The first ligand has τ = 10 s and is presented at 10^3 ligands. The second ligand has a dissociation time and ligand number denoted by the axes. The plot shows the percentage of TCRs occupied by the second ligand as a fraction of the total amount of bound TCRs. Parameters are the same as for a).

2 Model derivations

Each model of T cell activation described below has a different predictor of T cell activation, which we define to be R. We define $E_{\max}$ to be the value of R in the limit of excess pMHC ligand (e.g. $E_{\max} = \lim_{P_T \to \infty} R$) and define EC_{50} as the concentration of pMHC ligand that produces half-maximal R (e.g. value of P_T that satisfies $R = E_{\max}/2$).

2.1 Occupancy (Fig. 2A-C)

The occupancy model describes T-cell activation as being proportional to the concentration of bound TCR, which is defined as C and therefore in this model $R = C_T$. In this model pMHCs (P) can reversibly bind TCRs (T) to form a TCR-pMHC (C), see Fig. 2A. Using the principle of mass action, the kinetics are governed by the equation,

$$\frac{dC}{dt} = k_{\text{on}} PT - k_{\text{off}} C. \tag{1}$$

At equilibrium, $\frac{dC}{dt} = 0$ and

$$PT = K_{\text{D}} C, \tag{2}$$

where $K_{\text{D}} = k_{\text{off}}/k_{\text{on}}$. The total amount of peptide P_T and total amount of TCR T_T are conserved quantities given by the following conservation equations:

$$P_T = P + C \tag{3}$$
$$T_T = T + C. \tag{4}$$

Inserting the conservation equations into equation (2) gives,

$$C = \left(P_T + T_T + K_{\text{D}} - \sqrt{((P_T + T_T + K_{\text{D}})^2 - 4P_T T_T)}\right)/2. \tag{5}$$

2.1.1 Calculating $E_{\max}$ and EC_{50}

In this model $R = C$ and therefore $E_{\max}$ is the value of C in the limit of excess ligand (P_T). This can be found by non-dimensionalising the variables,

$$\hat{P} = \frac{P}{P_T}, \quad \hat{T} = \frac{T}{T_T}, \quad \hat{C} = \frac{C}{T_T},$$

and substituting these non-dimensionalised variables into the equations above to obtain,

$$\hat{P}\hat{T} = \frac{K_{\text{D}}}{P_T}\hat{C} \tag{6}$$
$$\hat{P} + \frac{T_T}{P_T}\hat{C} = 1 \tag{7}$$
$$\hat{T} + \hat{C} = 1 \tag{8}$$

Taking the limit of large P_T we obtain,

$$\lim_{P_T \to \infty} \hat{C} = 1$$

or in dimensional form,

$$E_{\max} = \lim_{P_T \to \infty} R = T_T.$$

To determine EC_{50} the concentration of P_T that satisfies the following relationship is determined,

$$R = E_{\max}/2$$
$$C = T_T/2.$$

By substituting the solution for C and solving for P_T we find that this concentration (defined as EC_{50}) is,

$$EC_{50} = K_{\mathrm{D}} + T_T/2 \tag{9}$$

2.2 Kinetic proofreading (Fig. 2D-F)

In this model a pMHC (P) can reversibly bind to a TCR (T) to form a complex (C_0). Upon forming a complex a series of chemical modifications can take place (C_i) that eventually produce a productive signaling complex (C_N). In this model, T cell activation is determined by the concentration of productive signaling complexes and therefore $R = C_N$. The parameters governing this model are the bimolecular binding rate (k_{on}), the unbinding rate (k_{off}), the modification rate (k_{p}), and the number of intermediate states (N). In this canonical kinetic proofreading model it is assumed that dissociation of pMHC from the TCR immediately reverses all TCR modifications.

This model is described by the following set of ODEs,

$$\partial P/\partial t = -k_{\mathrm{on}} PT + k_{\mathrm{off}} \sum_{i=0}^{N} C_i \tag{10}$$

$$\partial T/\partial t = -k_{\mathrm{on}} PT + k_{\mathrm{off}} \sum_{i=0}^{N} C_i \tag{11}$$

$$\partial C_0/\partial t = k_{\mathrm{on}} PT - (k_{\mathrm{off}} + k_{\mathrm{p}}) C_0 \tag{12}$$

$$\partial C_i/\partial t = k_{\mathrm{p}} C_{i-1} - (k_{\mathrm{p}} + k_{\mathrm{off}}) C_i \qquad \big(1 \leq i < N-1\big) \tag{13}$$

$$\partial C_N/\partial t = k_{\mathrm{p}} C_{N-1} - k_{\mathrm{off}} C_N \tag{14}$$

As before, we have the following conservation for pMHCs and TCRs,

$$P_T = P + C_T \tag{15}$$

$$T_T = T + C_T \tag{16}$$

where $C_T = \sum_{i=0}^{N} C_i$. We find an expression for C_T by substituting the conservation equations (15) and (16) into the steady-state of the ODE system,

$$C_T = \big(P_T + T_T + K_{\mathrm{D}} - \sqrt{(P_T + T_T + K_{\mathrm{D}})^2 - 4P_T T_T}\big)/2. \tag{17}$$

The next step is to relate C_N to C_T so that the magnitude of T-cell activation can be expressed as a function of P_T, T_T and K_{D}. At steady-state equation (14) becomes,

$$C_N = \frac{k_{\mathrm{p}}}{k_{\mathrm{off}}} C_{N-1}$$
$$= \frac{\alpha^N}{1-\alpha} C_0 \tag{18}$$

where $\alpha = k_{\mathrm{p}}/(k_{\mathrm{p}} + k_{\mathrm{off}})$. Next we can relate C_T to C_N using $C_i = \alpha C_{i-1}$ (equation 13 at steady-state),

$$\begin{aligned} C_T &= \sum_{i=0}^{N-1} C_i + C_N \\ &= \sum_{i=0}^{N-1} \alpha^i C_0 + C_N \\ \textit{(using geometric sum)} \qquad &= \Big(\frac{1-\alpha^N}{1-\alpha}\Big) C_0 + C_N \\ &= \frac{1}{\alpha^N} C_N. \end{aligned} \tag{19}$$

It follows that,

$$\mathrm{R} = C_N = \alpha^N C_T.$$

2.2.1 Calculating the $E_{\max}$ and EC_{50}

As before, we non-dimensionalise using $\hat{P} = P/P_T$, $\hat{T} = T/T_T$ and $\hat{C_T} = C_T/T_T$. The non-dimensionalised conservation equations are,

$$1 = \hat{P} + \frac{T_T}{P_T}\hat{C_T} \tag{20}$$

$$1 = \hat{T} + \hat{C_T}. \tag{21}$$

By substituting (20) and (21) into the steady-state non-dimensional form of equation (10) we get,

$$-k_{\mathrm{on}} P_T \hat{P}\hat{T} + k_{\mathrm{off}}\hat{C_T} = 0 \tag{22}$$

$$\hat{C_T} = \frac{P_T \hat{P}}{K_{\mathrm{D}} + P_T \hat{P}}. \tag{23}$$

When $P_T \to \infty$, we can see from equation (23) that,

$$\lim_{P_T \to \infty} \hat{C_T} = 1$$

and therefore,

$$E_{\max} = \lim_{P_T \to \infty} R = \alpha^N T_T.$$

To determine EC_{50} we solve for P_T in the following equation,

$$R = E_{\max}/2 \tag{24}$$

$$\alpha^N C_T = \alpha^N T_T/2. \tag{25}$$

and find that the value of P_T is,

$$EC_{50} = K_{\mathrm{D}} + T_T/2. \tag{26}$$

2.3 Kinetic proofreading with limited signalling (Fig. 2G-I)

To include limited signaling the kinetic proofreading model is modified to include a state whereby the productively signaling TCR-pMHC complex (C_N) may undergo a modification (with rate ϕ) that renders it non-signaling (C_N^-).

The ODE system governing this model is,

$$\partial P/\partial t = -k_{\text{on}}PT + k_{\text{off}}C_T \tag{27}$$
$$\partial T/\partial t = -k_{\text{on}}PT + k_{\text{off}}C_T \tag{28}$$
$$\partial C_0/\partial t = k_{\text{on}}PT - (k_{\text{off}} + k_{\text{p}})C_0 \tag{29}$$
$$\partial C_i/\partial t = k_{\text{p}}C_{i-1} - (k_{\text{p}} + k_{\text{off}})C_i \quad 1 \leq i < N-1 \tag{30}$$
$$\partial C_N/\partial t = k_{\text{p}}C_{N-1} - (k_{\text{off}} + \phi)C_N \tag{31}$$
$$\partial C_N^-/\partial t = \phi C_N - k_{\text{off}}C_N^- \tag{32}$$

where $C_T = \sum_{i=0}^{N} C_i + C_N^-$. As before, T cell activation is determined by C_N (i.e. $R = C_N$). At steady-state it can be seen that,

$$\begin{aligned} C_T &= \sum_{i=0}^{N-1} C_i + C_N + C_N^- \\ &= \frac{1-\alpha^N}{1-\alpha}C_0 + C_N + \frac{\phi}{k_{\text{off}}}C_N. \end{aligned} \tag{33}$$

By combining (28) with (29) at steady-state it can be seen that,

$$C_T = \frac{1}{1-\alpha}C_0. \tag{34}$$

Substituting this expression into equation (33) gives

$$C_N = \frac{k_{\text{off}}}{k_{\text{off}} + \phi}\alpha^N C_T. \tag{35}$$

2.3.1 Calculating the $E_{\max}$ and EC_{50}

As in the kinetic proofreading model, we find that $C_T \to T_T$ as $P_T \to \infty$. It follows that,

$$E_{\max} = \frac{k_{\text{off}}}{k_{\text{off}} + \phi}\alpha^N T_T. \tag{36}$$

Solving for P_T when $R = E_{\max}/2$ we find,

$$\text{EC}_{50} = K_{\text{D}} + T_T/2. \tag{37}$$

2.4 Kinetic proofreading with sustained signalling (Fig. 2J-L)

To include sustained signaling we modify the basic kinetic proofreading model by allowing TCRs that have reached the productively signaling state (C_N) to continue signaling even when pMHC dissociates (T^*). The rate that these productively signaling but unbound TCRs return to the unmodified state is determined by λ.

In this model, T cell activation is determined by both C_N and T^* and therefore $R = C_N + T^*$.

This model is described by the following system of ODEs,

$$\partial P/\partial t = -k_{\text{on}}PT + k_{\text{off}}\sum_{i=0}^{N} C_i - k_{\text{on}}PT^* \tag{38}$$

$$\partial T/\partial t = -k_{\text{on}}PT + k_{\text{off}}\sum_{i=0}^{N-1} C_i + \lambda T^* \tag{39}$$

$$\partial T^*/\partial t = k_{\text{off}}C_N - k_{\text{on}}PT^* - \lambda T^* \tag{40}$$

$$\partial C_0/\partial t = k_{\text{on}}PT - (k_{\text{off}} + k_{\text{p}})C_0 \tag{41}$$

$$\partial C_i/\partial t = k_{\text{p}}C_{i-1} - (k_{\text{p}} + k_{\text{off}})C_i \tag{42}$$

$$\partial C_N/\partial t = k_{\text{p}}C_{N-1} - k_{\text{off}}C_N + k_{\text{on}}PT^* \tag{43}$$

Using equation (40) at steady-state we can express the magnitude of T cell activation as a function of C_N,

$$T^* = \frac{k_{\text{off}}C_N}{k_{\text{on}}P + \lambda}.$$

and therefore,

$$\begin{aligned} R &= C_N + T^* \\ &= \left(\frac{k_{\text{on}}P + \lambda + k_{\text{off}}}{k_{\text{on}}P + \lambda}\right)C_N \\ &= \left(\frac{k_{\text{on}}(P_T - C_T) + \lambda + k_{\text{off}}}{k_{\text{on}}(P_T - C_T) + \lambda}\right)C_N. \end{aligned}$$

The parameter C_N must then be related to C_T so that T cell activation can be determined in terms of the variables T_T, P_T, and K_{D}. This can be done by substituting (41) into (39) to give,

$$-(k_{\text{off}} + k_{\text{p}})C_0 + k_{\text{off}}\sum_{i=0}^{N-1} C_i + \lambda T^* = 0. \tag{44}$$

Using the result,

$$C_T - C_N = \sum_{i=0}^{N-1} C_i = \left(\frac{1-\alpha^N}{1-\alpha}\right)C_0,$$

C_0 can be eliminated from (44) to eventually give,

$$C_N = \left(\frac{k_{\text{on}}P + \lambda}{\lambda + k_{\text{on}}P\alpha^N}\right)\alpha^N C_T. \tag{45}$$

T cell activation can now be determined as a function of C_T:

$$R = \left(\frac{k_{\text{on}}P + k_{\text{off}} + \lambda}{\lambda + \alpha^N k_{\text{on}}P}\right)\alpha^N C_T \tag{46}$$

$$= \left(\frac{k_{\text{on}}(P_T - C_T) + k_{\text{off}} + \lambda}{\lambda + \alpha^N k_{\text{on}}(P_T - C_T)}\right)\alpha^N C_T \tag{47}$$

where $C_T = \left(P_T + T_T + K_{\text{D}} - \sqrt{(P_T + T_T + K_{\text{D}})^2 - 4P_T T_T}\right)/2$.

2.4.1 Calculating the $E_{\max}$ and EC_{50}

As before, the non-dimensionalised variables are $\hat{P} = P/P_T,\ \hat{T} = T/T_T,\ \hat{T^*} = T^*/T_T,\ \hat{C}_i = C_i/T_T$. The non-dimensionalised conservation equations become,

$$1 = \hat{P} + \frac{T_T}{P_T}\hat{C_T} \tag{48}$$

$$1 = \hat{T} + \hat{T^*} + \hat{C_T}. \tag{49}$$

To calculate the $E_{\max}$, equation (46) can be written in terms of non-dimensionalised variables,

$$\begin{aligned} R &= \left(\frac{k_{\text{on}}P_T\hat{P} + k_{\text{off}} + \lambda}{\lambda + \alpha^N k_{\text{on}}P_T\hat{P}}\right)\alpha^N T_T\hat{C_T} \\ &= \left(\frac{k_{\text{on}}P_T\hat{P} + k_{\text{off}} + \lambda}{\lambda + \alpha^N k_{\text{on}}P_T\hat{P}}\right)\alpha^N P_T(1-\hat{P}) \\ &= \left(\frac{k_{\text{on}}P_T\hat{P} + k_{\text{off}} + \lambda}{\lambda + \alpha^N k_{\text{on}}P_T\hat{P}}\right)\alpha^N P_T(1 - \frac{-(K_{\text{D}} - P_T + T_T) + \sqrt{\left(K_{\text{D}} - P_T + T_T\right)^2 + 4P_T K_{\text{D}}}}{2P_T}) \end{aligned}$$

In the limit of excess P_T we find,

$$E_{\max} = \lim_{P_T \to \infty} R = T_T$$

The concentration of P_T at half the maximal response can be found by solving for P_T in the equation $R = T_T/2$. This leads to,

$$T_T/2 = \left(\frac{k_{\text{on}}(P_T - C_T) + k_{\text{off}} + \lambda}{\lambda + \alpha^N k_{\text{on}}(P_T - C_T)}\right)\alpha^N C_T,$$

where $C_T = \left(P_T + T_T + K_{\text{D}} - \sqrt{(P_T + T_T + K_{\text{D}})^2 - 4P_T T_T}\right)/2$, which can be rearranged to give,

$$P_T = \frac{\alpha^N C_T(k_{\text{off}} + \lambda - k_{\text{on}}C_T + k_{\text{on}}T_T/2) - T_T\lambda/2}{\alpha^N k_{\text{on}}(T_T/2 - C_T)}, \tag{50}$$

Note that this expression implicitly depends on P_T through C_T and therefore to determine the EC_{50} this equation must be numerically solved for P_T.

2.5 Summary of analytical results

Definitions: $\alpha = k_p/(k_p + k_{off})$, T_T is the total concentration of TCR, P_T is the total concentration of pMHC, and C_T is the total concentration of bound TCR and is given by $C_T = \left(P_T + T_T + K_D - \sqrt{(P_T + T_T + K_D)^2 - 4P_T T_T}\right)/2$ where $K_D = k_{off}/k_{on}$.

Occupancy (Fig. 2A-C)
T-cell activation is proportional to the concentration of bound TCR-pMHC complexes ($R = C_T$).

$$R = C_T$$
$$EC_{50} = K_D + T_T/2$$
$$E_{max} = T_T$$

Kinetic proofreading (Fig. 2D-F)
T-cell activation is proportional to the concentration of competently signaling TCRs ($R = C_N$).

$$R = \alpha^N C_T$$
$$EC_{50} = K_D + T_T/2$$
$$E_{max} = \alpha^N T_T$$

Kinetic proofreading with limited signalling (Fig. 2G-I)
T-cell activation is proportional to the concentration of competently signaling TCRs ($R = C_N$).

$$R = \left(\frac{k_{off}}{k_{off}+\phi}\right)\ \alpha^N C_T$$
$$EC_{50} = K_D + T_T/2$$
$$E_{max} = \frac{k_{off}}{k_{off}+\phi}\ \alpha^N T_T$$

Kinetic proofreading with sustained signalling (Fig. 2J-L)
T-cell activation is proportional to the concentration of competently signaling TCRs ($R = C_N + T^*$).

$$R = \left(\frac{k_{on}(P_T - C_T) + k_{off} + \lambda}{\lambda + \alpha^N k_{on}(P_T - C_T)}\right) \alpha^N C_T$$
$$EC_{50} = \frac{\alpha^N C_T (k_{off} + \lambda - k_{on} C_T + k_{on} T_T/2) - T_T \lambda/2}{\alpha^N k_{on}(T_T/2 - C_T)}$$
$$E_{max} = T_T$$

3 Co-presentation of peptides

The phenotypic models described above can be modified to predict T cell activation when two different pMHC are presented (Fig. 5). Note that explicit expressions for $E_{\max}$ and EC_{50} are not determined but instead we numerically solve for the predictor of T cell activation (R) in each case.

3.1 Occupancy model

When two pMHC are co-presented (denoted as P_1 and P_2), we have the following equilibrium equations,

$$P_1T = k_{1D}C_{1T} \tag{51}$$
$$P_2T = k_{2D}C_{2T}. \tag{52}$$

and conservation equations:

$$P_{1T} = P_1 + C_{1T} \tag{53}$$
$$P_{2T} = P_2 + C_{2T} \tag{54}$$
$$T_T = T + C_{1T} + C_{2T} \tag{55}$$
$$C_T = C_{1T} + C_{2T}. \tag{56}$$

Equations (51) and (52) can be combined to give:

$$k_{1D}k_{2D}(C_{1T} + C_{2T}) = k_{1D}P_2(T) + k_{2D}P_1(T) \tag{57}$$
$$k_{1D}k_{2D}C_T = k_{1D}P_2(T_T - C_T) + k_{2D}P_1(T_T - C_T). \tag{58}$$

Equations (51), (53) and (55) can be used to give the expression,

$$P_i = \Big(\frac{k_{iD}}{k_{iD} + T_T - C_T}\Big)P_{iT}. \tag{59}$$

This can be substituted into (58) to eventually give:

$$(k_{1D} + T_T - C_T)(k_{2D} + T_T - C_T)C_T =$$
$$(k_{1D} + T_T - C_T)(T_T - C_T)P_{2T} + (k_{2D} + T_T - C_T)(T_T - C_T)P_{1T}.$$

This can be simplified as follows,

$$\begin{aligned} &C_T^3 - \big(P_{1T} + P_{2T} + 2T_T + k_{1D} + k_{2D}\big)C_T^2 \\ &+ \big((k_{1D} + T_T)(k_{2D} + T_T) + P_{2T}(2T_T + k_{1D}) + P_{1T}(2T_T + k_{2D})\big)C_T \\ &+ P_{2T}(k_{1D}T_T + T_T^2) + P_{1T}(k_{2D}T_T + T_T^2) = 0. \end{aligned} \tag{60}$$

To determine C_T we numerically solve this cubic equation using the Matlab (Mathworks, MA) function *fsolve*. In order to check this derivation, it can be seen that when $P_{2T} = 0$ equation (60) becomes:

$$\begin{aligned} &C_T^3 - \big(P_{1T} + 2T_T + k_{1D} + k_{2D}\big)C_T^2 + \big((k_{1D} + T_T)(k_{2D} + T_T) + P_{1T}(2T_T + k_{2D})\big)C_T + P_{1T}(k_{2D}T_T + T_T^2) \\ &= (C_T - k_{2D} - T_T)(C_T^2 - (k_{1D} + P_{1T} + T_T)C_T + T_TP_{1T}) \\ &= 0. \end{aligned}$$

Since $C_T \leq T_T$ we can see that $C_T = k_{2D} + T_T$ cannot be a solution and therefore,

$$C_T^2 - (k_{1D} + P_{1T} + T_T)C_T + T_TP_{1T} = 0, \tag{61}$$

which is the equation for C_T for a single peptide, as in (17).

3.2 Kinetic proofreading

Now that an expression C_T as a function of P_{1T}, P_{2T}, k_{1D}, k_{2D} and T_T has been found, it can be seen using (51) and (55) that:

$$C_{iT} = \frac{P_{iT}(T_T - C_T)}{k_{iD} + T_T - C_T}. \tag{62}$$

And so from (19), it can be seen that the amount for each peptide in the final signalling state C_{iN} is,

$$C_{1N} = \alpha_1^N C_{1T} \tag{63}$$
$$C_{2N} = \alpha_2^N C_{2T} \tag{64}$$

where $\alpha_i = \frac{k_{\mathrm{p}}}{k_{\mathrm{p}}+k_{\mathrm{offi}}}$. Therefore, T cell activation in this model can be determined as follows,

$$R = C_{1N} + C_{2N}. \tag{65}$$

3.3 Kinetic proofreading with limited signalling

Assuming that the rate ϕ of transferring from the productively signaling state (C_N) to the inert state (C_N^-) is the same for both pMHCs, then following from (35) and (62) it can be seen that,

$$C_{1N} = \frac{k_{\mathrm{off1}}}{k_{\mathrm{off1}} + \phi}\alpha_1^N C_{1T} \tag{66}$$
$$C_{2N} = \frac{k_{\mathrm{off2}}}{k_{\mathrm{off2}} + \phi}\alpha_2^N C_{2T}. \tag{67}$$

and as before, T cell activation in this model can be calculated using,

$$R = C_{1N} + C_{2N}. \tag{68}$$

3.4 Kinetic proofreading with sustained signalling

In this model, T cell activation is determined as follows,

$$R = C_{1N} + C_{2N} + T^*. \tag{69}$$

The expressions for C_{1N} and C_{2N} are,

$$C_{1N} = \left(\frac{k_{\mathrm{on}}(P_{1T} - C_{1T}) + \lambda}{\lambda + \alpha_1^N k_{\mathrm{on}}(P_{1T} - C_{1T})}\right)\alpha^N C_{1T} \tag{70}$$
$$C_{2N} = \left(\frac{k_{\mathrm{on}}(P_{2T} - C_{2T}) + \lambda}{\lambda + \alpha_2^N k_{\mathrm{on}}(P_{2T} - C_{2T})}\right)\alpha^N C_{2T}. \tag{71}$$

In order to find the expression for T^* we use the equivalent of equation (40) when two pMHC are presented,

$$\partial T^*/\partial t = k_{\mathrm{off1}}C_{1N} + k_{\mathrm{off2}}C_{2N} - k_{\mathrm{on}}(P_1 + P_2)T^* - \lambda T^*.$$

At steady-state we find,

$$T^* = \frac{k_{\mathrm{off1}}C_{1N} + k_{\mathrm{off2}}C_{2N}}{k_{\mathrm{on}}(P_{1T} - C_{1T} + P_{2T} - C_{2T}) + \lambda}. \tag{72}$$

References

1. P. Francois, G. Voisinne, E. D. Siggia, G. Altan-Bonnet, and M. Vergassola. PNAS Plus: Phenotypic model for early T-cell activation displaying sensitivity, specificity, and antagonism. *Proceedings of the National Academy of Sciences*, Feb. 2013.

Supplementary Figure

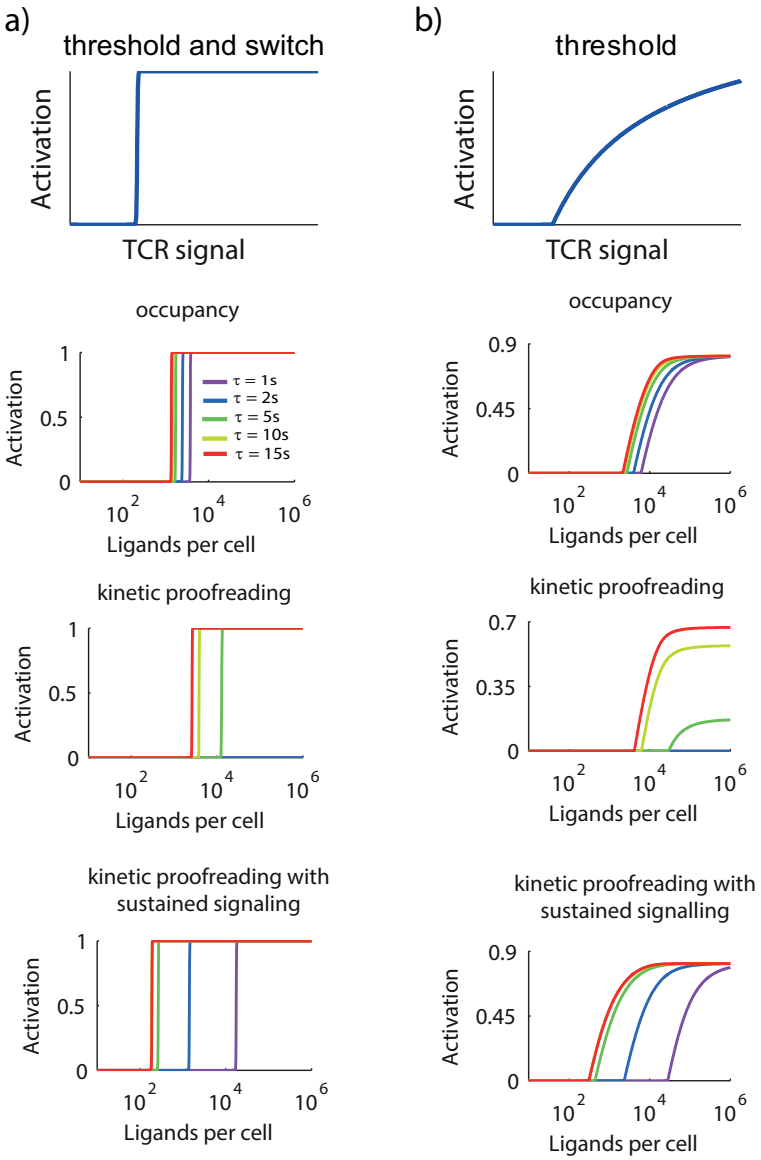

Figure S1: Effect of thresholds and switches on phenotypic models not shown in Fig. 4.

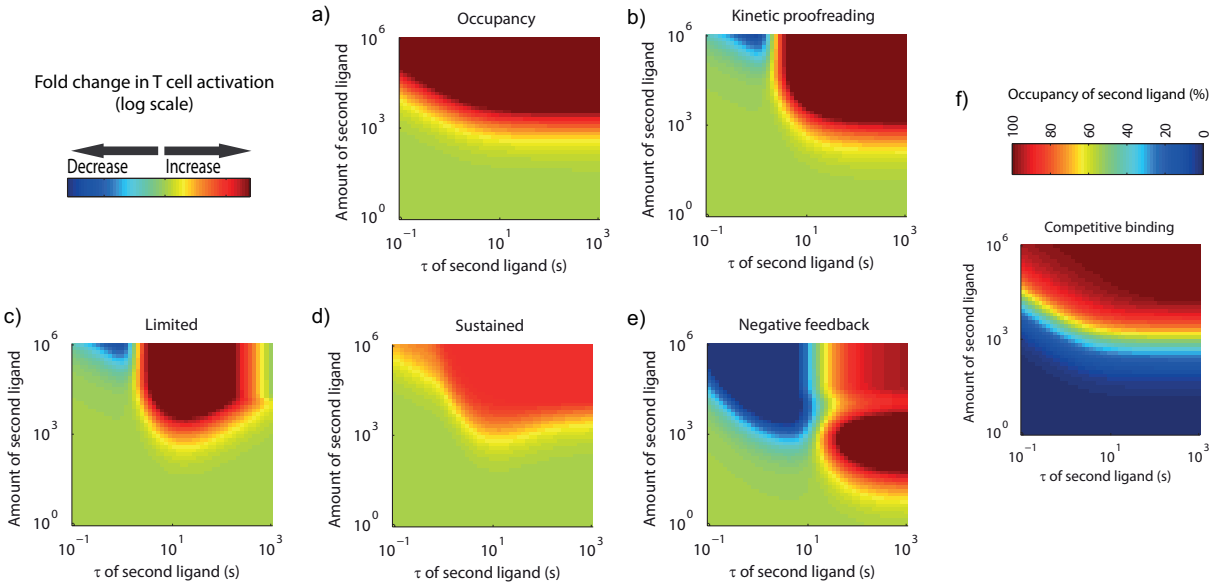

Figure S2: Effect of co-presentation of a second pMHC on T cell activation. A-E) Shown are heat maps of the fold change in T cell activation (on a log-scale) over the dissociation time (x-axis) and the number of ligands (y-axis) for the second pMHC. The first ligand is presented at a fixed number of 1000 per cell with a dissociation time of 10 s. F) Shown is the percentage of TCRs occupied by the second ligand. The calculations shown in Fig 6 are slices of these heat maps when the second pMHC is presented at 1000 ligands per cell.